REPORT NO. 147

May, 1961.

THE COLLEGE OF AERONAUTICS

CRANFIELD

Buckling due to Thermal Stress of Cylindrical Shells Subjected to Axial Temperature Distributions

- by -

D. J. Johns, M.Sc.(Eng.), M.I.Ae.S.
D. S. Houghton, M.Sc.(Eng.), A.M.I.Mech.E., A.F.R.Ae.S.
J. P. H. Webber, D.C.Ae.

SUMMARY

Thermal stress distributions in uniform circular cylindrical shells due to axial temperature distributions are investigated. The discontinuity effect due to the presence of a cooler stiffening bulkhead is considered, and the possibility of thermal buckling of the shell due to the circumferential discontinuity stress is examined. The buckling analysis is based on Donnell's shell equation, and particular attention is given to shells having clamped edges.

An experimental investigation of this buckling problem is discussed, and the results obtained are seen to agree reasonably well with theory.

REPORT NO. 147

THE COLLEGE OF AERONAUTICS

CRANFIELD

CORRIGENDA

Page 2, Equation 2.4 $\theta_o =$ Not $Q_o =$

Page 4, Section 4. Figs. 1 and 2 Not Figs. 1 and 3.

CONTENTS

		Page
	Summary	
	Notation	
1.	Introduction	1
2.	The Basic Displacement Equations	1
3.	Thermal Displacements in Unstiffened Shells	2
	3.1. Polynomial Temperature Distributions	2
	3.2. Trigonometric Temperature Distributions	3
4.	Thermal Displacements and Stresses in Plane Bulkheads	4
5.	Thermal Displacements and Stresses in Shells Stiffened by Plane Bulkheads	5
	5.1. The General Discontinuity Problem	5
	5.2. Results for Simple Configurations	7
6.	Thermal Buckling of Circular Cylindrical Shells	10
	6.1. Clamped Edge Circular Cylinders	11
	6.2. Simply Supported Circular Cylinders	13
7.	Application of the Theory	13
	7.1. Uniform Shell Temperature Rise	13
	7.2. Clamped Edge Cylinder with Non-Uniform Shell Temperature Rise	14
8.	Experimental Investigation of a Clamped Circular Cylinder	14
	8.1. Description of Specimen	14
	8.2. Instrumentation	15
	8.3. Heating Apparatus	15
	8.4. Description of Experiments and Results	15
9.	Conclusion	16
10.	References	17
	Appendix A - Transient Temperature Prediction for Arbitrary Heating of a Shell-Bulkhead Configuration	19
	Appendix B - Thermal Stresses for Assumed Temperature Distributions	25
	Appendix C - Thermal Buckling of Clamped Cylindrical Shell (first order solution)	28

Contents (Continued)

Table 1 - General Thermal Buckling Determinant

Table 2 - Symmetric Buckling Determinant

Table 3 - Notation for Tables (1) and (2)

Figures

NOTATION

n	Number of cycles experienced at a given level of stress
N	Number of cycles to failure, at a given level of stress
R	Ratio of cycles experienced, to cycles to failure, at a given level of stress or load, called the cycle ratio
S	Alternating stress, or stress amplitude used in a fatigue cycle. When the word "stress" is used alone, it denotes alternating stress
S_m	Mean stress of the fatigue cycle
S_{max}, S_{min}	The maximum, minimum value of stress in a fatigue cycle
D	The damage quantity, a function of cycle ratio R defined further where it appears
lg	Unaccelerated level flight condition where unit acceleration (32.2 feet/sec./sec.) exists everywhere in the region concerned
U	Gust velocity in feet per second equivalent airspeed (Br. definition)
F_c	Cycle-based factor used in life assessment calculations
h	Crack depth
E	Endurance limit, (in terms of stress amplitude)
y_m	Gust velocity function for zero log cycles; i.e. for one cycle of fatigue
σ	The relative air density
b, c, C, k, m, A, K	Constants used in this work
S-N or SN	The general relation between alternating stress level and endurance for a material tested under constant amplitude fatigue cycles
Partial Damage	- Two-level constant amplitude fatigue tests where the first stress level is run continuously to its completion, and the specimen tested to destruction at the second level of alternating stress
Element	- A single non-redundant structural member which fails when it is fractured in fatigue, as opposed to a redundant structure which is only weakened when one of its elements fails. This is the only type of structure having a fatigue "life" in the usual sense

Notation (Continued)

The Static Axis - The $\frac{1}{4}$ cycle line on a normal plot of the S-N relation

In general, where special notation is used in a single particular section of the report, the terms are defined in that section as they are used.

1. Introduction

The simple linear law of cumulative damage in fatigue fails to take account of healing and damaging effects. Various investigators have introduced more complex relationships in an attempt to include such effects, but unfortunately the results are no more representative of what happens to an aircraft in service than are those of the linear law.

In this work, a new approach has been made in that the behaviour of the material under repeated stress is shown to fall into three different stress regions. In the intermediate stress region it appears that cumulative damage does follow a linear law. Outside this intermediate region non-linear damage modifies the fundamental behaviour, and from an analysis of experimental results the non-linear functions have been estimated. The modified linear law is then applied to the determination of the fatigue behaviour of a particular aircraft project.

2. Existing Theories of Cumulative Damage

The Linear Cumulative Damage Law

This simple, widely known and used hypothesis owes its origins to a number of investigators. Miner, however, is probably chiefly responsible for bringing it to the attention of the aeronautical world.

The rule, as he stated it in Ref. 1, is:

> "Damage could be expressed in terms of the number of cycles applied, divided by the number to produce failure at a given stress level. When the summation of these increments of damage at several stress levels became unity, failure occurred".

Thus, if W_1 is the net work absorbed at failure at N_1 cycles by a specimen loaded sinusoidally at constant amplitude at a given stress level S_1, and if w_1 is the work done in n_1 cycles, then, assuming work is absorbed (i.e. damage is accumulated) at a rate linearly proportional to the number of cycles applied:

$$\frac{w_1}{W_1} = \frac{n_1}{N_1}$$

(This law will henceforth be called the linear rule due to its linear relation with cycle ratio).

If damage accumulation is independent of stress level, then summing over the stress levels:

$$\Sigma \frac{w}{W} = \Sigma \frac{n}{N}$$

If no work hardening occurs, let the total work that can be absorbed by the specimen be tantamount to failure.

$$\text{i.e.} \quad \Sigma \frac{w}{W} = 1 \quad \text{at failure}$$

$$\text{Thus} \quad \Sigma \frac{n}{N} = 1 \quad \text{denotes failure of the part}$$

This rule can be evolved, without the work assumptions, merely from the statements:

(1) Damage depends upon a single parameter, the cycle ratio

(2) The fatigue process is relatively the same at every stress level, as has been done in Ref. 2.

By summing increments of travel along two affine fatigue crack growth curves, F. R. Shanley in Ref. 3 arrived at the linear rule in an indirect manner. The destination of his train of thought was inevitable, however, for while he attached great importance to the particular form of his crack growth curve, it can be shown that it is almost immaterial what form the curve may take. As long as the curves are non-dimensionally invariant with stress, (i.e. affine), and proportional in some way to the cycle ratio (as this work is) the linear rule will follow. The following figure shows how the accumulation of damage is proposed to take place:

A stress S_1 is applied for Δn_1 cycles, after which stress S_2 is applied for Δn_2 cycles. This load spectrum is repeated until failure - denoted by the attainment of an arbitrary crack depth - occurs at N_p cycles.

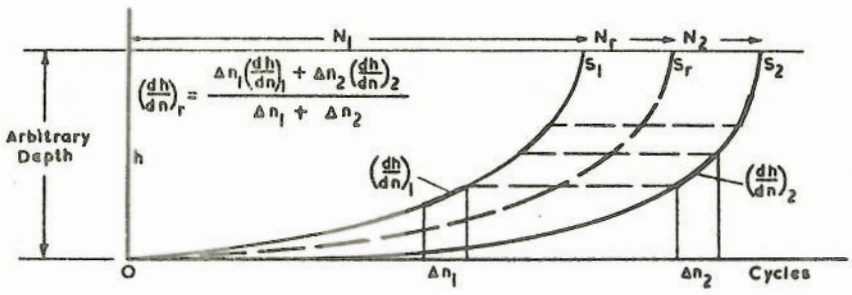

FIG. A.

The actual form of the final relation is given in terms of a reduced stress, $S_r = \left[\frac{\Sigma \Delta n S^x}{\Sigma \Delta n} \right]^{\frac{1}{x}}$ where x is the reciprocal of the slope of the best straight line through the S-N curve when plotted on log stress - log cycles paper.

Deficiencies

An examination of a great number of reports reveals the following four main deficiencies of the beautifully simple linear rule.

(1) The rate of damage accumulation is not a simple linear function of cycle ratio, but a complex relation exists which is dependent on stress level, sequence of loads, and type of loading.

(2) Previous history has an enormous effect on the summation. This is not accounted for, and values have ranged "from 0.18 to 23.0 with only a small portion giving the assumed value of unity". (Ref. 4).

(3) There is no provision for beneficial effects as can be obtained from certain applications of single preloads (Ref. 5) or of large numbers of ultra-low stress level cycles which have actually improved on the single-level lives in many studies, including the present one.

(4) As the rule is dependent on cycle ratio as obtained from the S-N curve, those stress levels below the level at which the S-N curve flattens out, are inadequately represented. As Dr. Gassner points out in Ref. 6, "In contradistinction to the view expressed in British literature, (these levels) play an active part in the formation of fatigue fractures". Many researchers, such as Ref. 7, have shown very appreciable differences in lives obtained by including and then excluding low level cycles which predominate in numbers in the gust traces taken from actual flights.

An interesting and quite popular notion has grown out of the lack of appreciation of the final point, in the idea of "most damaging stress levels".

The mixture of both healing and damaging effects is evident from the fact that averaging of many summation values over, say, the stress range often results in an answer close to unity. This seems to indicate that the linear law is truly part of the story, but that there exist non-linear effects which are not accounted for.

To conclude, it has become increasingly evident that the widely used linear theory does not provide a sufficiently close approximation to the real rather complex and probably non-monotonic progress of fatigue damage under varying stress amplitudes. How could it, when it is defined by only a single parameter like the cycle ratio ?

Cumulative Damage by Empirical Two-Level Relations

A great number of investigators (Refs. 8 - 12) have tried to clear up the mystery of damage accumulation by studying carefully the effect of a given stress level upon a second level, by partially running the specimen at constant load amplitude at the first level and then running the specimen to failure at the second level. By defining 100% damage as given by the utilization of unity in total cycle ratio, other quantities of damage can be found by failure at other values of cycle ratio, from relation of the

cycles at failure to the cycles to failure if only the second level was tested. For example, a specimen tested to 0.5 cycle ratio at the first stress level, which then fails half-way to the single-level cycles-to-failure at the second level, has endured a total of 0.75 cycle ratio and accumulated 0.50 of the nominal damage.

Some examples of the general results are given in the following diagram :

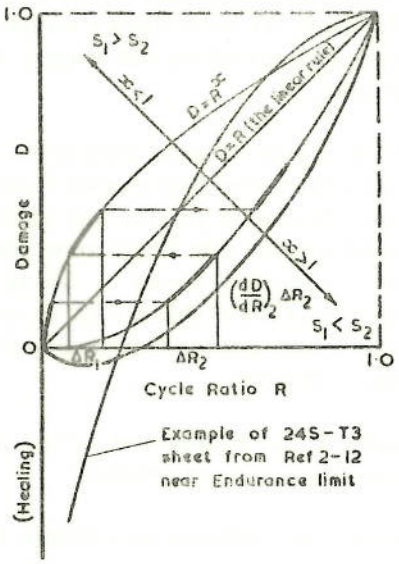

$$\Delta D = \left(\frac{dD}{dR}\right)_1 \Delta R_1 + \left(\frac{dD}{dR}\right)_2 \Delta R_2$$

$$(R)_{D=1} = \int_0^1 \frac{\Delta R_1 + \Delta R_2}{\left(\frac{dD}{dR}\right)_1 \Delta R_1 + \left(\frac{dD}{dR}\right)_2 \Delta R_2} \cdot dD$$

FIG. B.

In general the interaction of two levels results in a power relation between the fraction of cycle ratio used and the fraction of nominal (single level) damage obtained. One such relation is given by the finite power series:

$$\Sigma \frac{n}{N} = 1 + \frac{n_1}{N_1} - \left(\frac{n_1}{N_1}\right)^2$$

for two level tests with L.65 from Ref. 11. Here, the questionable ordinate "Percent Damage" was replaced by the more honest label "Subsequent cycle ratio for Failure". D.L.Henrey in Ref. 13 has been able to develop this approach to adequately account

for two-level behaviour of the endurance limit with steel.

This approach avoids the use of affine curves but instead uses a questionable quantity called Percent Damage to obtain non-affine curves from which to form a cumulative damage summation technique based on summing the projections of these damage curves. Unfortunately this method is restricted to the particular stress levels and cycle ratios investigated as there seem to be no observations thus far of a general nature.

As this method is an empirical study of the interactions of stress levels, a prohibitive amount of testing is necessary to cover all the combinations of stress levels that will be met in service. The major difficulty, however, is that two-level fatigue is almost never met with in service. Studies reveal that there is often no correlation between two-step tests of this type, where all the cycles at the first level are completed before moving to the second level, and two-level programme tests, where the levels are alternated but with the same equivalent cycle ratios at failure. This two-level approach, like the others discussed so far, actually relies on a single parameter, the remaining endurance at the second stress level. It is therefore impossible to define contributions from one level to another at stresses below the endurance limit even though they have been proved to contribute to failure in multi-level tests. Extending this approach to the practical cases of many stress levels is an almost impossible complication. Even extension to three stress levels results in families of irregular surfaces in a three-dimensional damage plot (Ref. 12). In short, this approach tends to be descriptive, but not very explanatory in nature.

Cumulative Damage by Power-Weighting the Stress Levels

(a) When Professor F. R. Shanley observed that the affine curve relation obtained the linear rule, he studied test results and concluded that the linear rule tended to under-estimate the damage contribution at high stresses. Re-examining the equations, he obtained a new rule called the 2 x method, which merely power-weights the contributions according to stress level in a uniform manner. This has been found to be too severe a 'solution' and at any rate its source is quite obscure, for Schijve writes in Ref. 14:

> "The derivation given in (Ref. 3) is incomplete and it must be concluded that it either contains an error, or is based on some additional assumption which has not been mentioned".

An algebraic check by the author using the reference directly confirms this viewpoint. The final form of the 2 x equation is also given in terms of a reduced stress S_r similar to the affine relation.

$$S_r = \left[\frac{\Sigma \Delta n \, s^{2x}}{\Sigma \Delta n} \right]^{\frac{1}{2x}}$$

From a detailed study of damage behaviour, it appears that overall corrective measures such as this add little to our knowledge of fatigue. A consideration of the deficiencies of the linear rule shows that such crude and severe measures only tend to obscure the actions of the various contributory effects.

(b) Marco and Starkey in Ref. 10 studied two-level fatigue results using 75 S-T Aluminium Alloy. They concluded that the dependence of damage on stress level could be given by the cycle ratio, as in the linear rule, above a certain critical stress level marking the change in fatigue crack formation from a single crack at low stress levels to many cracks at high stress levels, and by the square of the cycle ratio below this critical stress. This critical stress level lies in the intermediate range of the S-N curve for this material. Professor Miles, in Ref. 15, studied random loading using this criterion, to compare it with linear rule results, and found relatively small changes "compared with experimental scatter". He considers therefore that the linear rule is adequate for random loading. This, however, can be generally refuted. This rule, then, seems to be inadequate to account for the deficiencies of the linear merely by dividing the whole S-N curve into two parts. It does, however, represent a slight improvement over the Shanley 2 x method in that it recognizes that the damage function is not uniform in its dependence on the stress level.

Cumulative Damage with Stress Interaction Factors

Professor A. M. Freudenthal, in Ref. 16, has developed a generalized damage relation based on the summation of cycle-ratio functions raised to a power which varies in a general way with stress level. Fracture is defined in the usual way; i.e. when the summation is unity.

He then extends this to include stress interaction effects. This can only be done, of course, if the process is truly random as the damage is a non-linear function depending on stress level, and any well-defined sequence will give its own particular result. He then introduces a factor which willbe a function of stress levels and of the relative frequency of stress which is then applied to the general equation. He suggests, from experimental evidence, that the interaction factor will be near unity for high stresses, and near ten for stresses close to the endurance limit. Because of these powerful sequential effects, he states "that stress interaction effects of such magnitude reduce to practical insignificance the possible effects of non-linearity of the damage rate".

The approach adopted by Professor Freudenthal is undoubtedly the most promising yet encountered, for it deals adequately with non-linear damage accumulation, and perhaps adequately with sequence effects. However, it suffers from a lack of simplicity which may be remedied later when more random test results are available.

It is clear, therefore, from these alternative theories that the linear rule is very useful as it is, and the author is convinced that no radical alternative will be found. While tne four deficiencies of the linear rule must be adequately remedied, everything should be done to retain as much as possible of its simplicity.

3. Improving the Linear Rule

Characteristics of the S-N Relation

In Ref. 17, Weibull has shown that, under certain conditions, the whole S-N relation plotted on a semilog basis can be transformed into a single straight line on a plot of stress versus (cycles)$^{-c}$ i.e. a reciprocal plot of cycles. This occurs when the parameters match in the equations.

$$N = k(S - E)^{-m} \quad \text{for the low stress levels} \tag{1}$$

$$N + B = KS^{-m} \quad \text{for high stress cycles} \tag{2}$$

where B is a parameter which must be taken into account when dealing with the high stress region of the S-N curve. Lundberg in Ref. 18, omits this parameter and combines the equations (1) and (2) in the form

$$N = \alpha(S - E)^{-\beta} \tag{3}$$

where α and β are constants, stating that :

> "For the fatigue of aircraft structures due to gust loads, the damage caused by the high loads corresponding to the lefthand part of the endurance curve is usually negligibly small, and then the simpler form of the equation can be used".

Equation (3) can be expressed in the form:

$$S = b\,N^{-c} + E \tag{4}$$

While the above argument may be true where stress concentrations are beneficially affected by high loads, it has not been found true with plain specimens, as the test results of Appendix I show. On the contrary, most research so far confirms that high loads play a very significant part in the accumulation of fatigue damage.

The above simplification has serious shortcomings.

(1) The matching of parameters is quite rare. Weibull states that as a rule the two curves are not amenable to such 'integration'. The author has carried out this plotting for the test data and a narrow S-N curve results.

(2) There is nothing to account for the effects which contribute to damage accumulation below the endurance limit.

(3) There is evidence that crack initiation follows an exponential law and not a reciprocal law. While this does not appear significant at first sight, it will be seen shortly that the crack growth equation yields the fundamental relation between stress level and endurance.

There is always a certain amount of arbitrary smoothing out of the curve joining endurance means at different stress levels. With this latitude in drawing S-N curves, the assumption has tacitly grown over the years that the S-N relation is essentially made up of two parts, as given in the equations (1) and (2), which join at an inflection point at an intermediate stress level. In fact, life assessment formulae have been built upon an S-N equation fitting the lower half of the curve only, coupled with the linear rule (Ref. 18).

One of the most common complaints has been that the linear rule underestimates damage effects at high stress levels. This complaint and the deficiencies of the linear rule enumerated in the previous section have led the author to suspect the above assumption, and to examine this aspect of endurance curves in detail.

Choice of Plot

Some workers argue that the S-N relation should be plotted linearly in both directions. This gives the truest picture of the actual nature of the curve, with the enormous increase in endurance and in scatter that takes place at low stress levels. The plot is not satisfactory, for to be practical the endurance scale must be condensed and the behaviour at stresses above the endurance limit is then difficult to assess.

The best plot for the S-N curve is that which makes the fundamental process stand out clearly, and in a manner amenable to study. Toward this end, Professor F. R. Shanley, in Ref. 3, suggests the log - log plot which also appears to resolve the S-N curve into a single straight line, and he has drawn attention to fatigue crack initiation as the process to be made amenable to study. He has developed an exponential crack growth equation which leads to a linear relation for the log - log plot. This then leads to a damage accumulation law which would apply to the whole S-N relation, since many data make it appear linear in this plot. Unfortunately his relation has been shown to be an indirect form of the linear rule, and no progress seems possible past this point at present.

The semilog plot, on the other hand, appears promising to the author for the following reasons:

(a) Exponential crack growth equations can lead to a semilog plot of stress-log cycles, as well as the log stress-log cycles plot, as will be shown shortly.

(b) There is evidence pointing to a division of the S-N relation into three areas of behaviour wherein the middle region has 'ideal' characteristics. With the concept of three areas in mind, nearly all the S-N data can be plotted in three sections of which the centre section is linear, in a semilog plot.

(c) The relative frequency of random forces can be accurately represented by a straight line on a semilog plot. A really significant gain in simplicity should then be possible if the fundamental behaviour of fatigue also consists of a straight line relation in this plot.

(d) From a purely practical standpoint, the vast majority of S-N data are plotted on this form of scale.

The following diagram shows the notation which will be used to identify the three areas of behaviour:

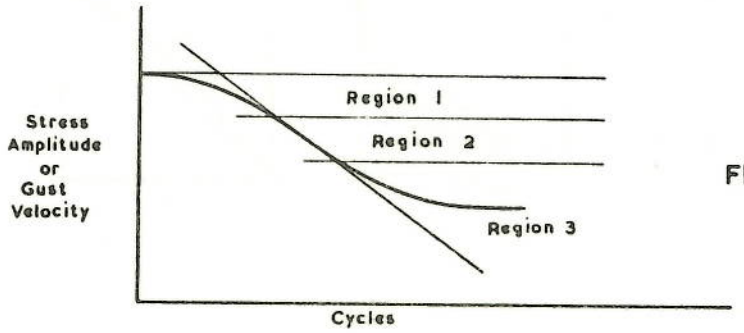

FIG. C.

Region (1): This region, of high alternating stresses, is characterized by the convex-upwards section of the curve. Reports on plain specimens seem to agree that this is an area where the rate of change of damage activity with stress is severe and non-linear. Multiplicity of crack nuclei and other characteristics of high stress level fatigue fracture all point to the accumulation of damage in a severe manner. From the characteristic gradual curving of the S-N relation it appears that the non-linear effect is a gradual one increasing in frequency with stress level, until nearly all specimens fail at very low endurance just below the static ultimate. This region will be called the region of non-linear damage.

Region (2): This region comprises that part of the finite-endurance S - Log N relation in which the test data appear to fall in a straight line. This is the intermediate stress level region commonly considered the region around the point of inflection in present-day fatigue research. This region is characterized then by a constant change in the damage rate with stress level, and will be called the linear region.

Region (3): This low-stress level region is characterized by a slackening off of the damage activity in which a random healing effect allows more and more specimens to withstand the fatigue indefinitely, as the stress level is lowered. This region will be called the healing region.

Evidence from Two Level Damage Tests

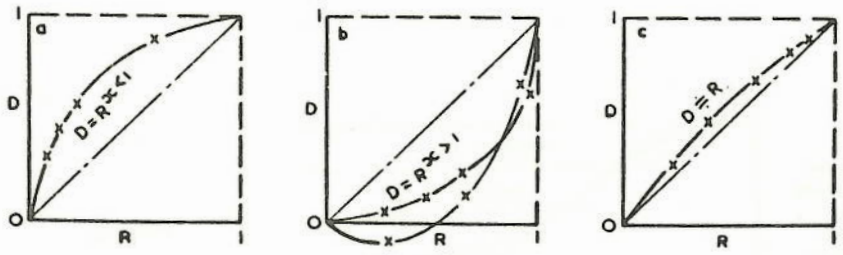

FIG. D.

The figure above shows what are perhaps the only general features of the results from two-level damage tests.

(a) If $S_1 > S_2$, damage, defined in degree by the remaining endurance at S_2, proceeds rapidly at first, and then slowly as the cycle ratio increases. The damage function thus follows a curve of the family $D = R^x$ where $x < 1$, and the greater S_1 is in comparison with S_2 the further the resulting curve of results deviates from the straight line given by the straight line $D = R$. (i.e. x decreases toward zero).

(b) If $S_1 < S_2$ damage proceeds slowly, then rapidly as cycle ratio increases. The damage function follows a curve of the family $D = R^x$ where $x > 1$ and the lower S_1 is compared with S_2 the further the curve moves from the straight line $D = R$ (and x increases rapidly). Also in nearly all cases where a beneficial healing effect is encountered (i.e. where the run at S_1 actually improves on the single level endurance at S_2), the effect is a deviation of this curve to points below the $D = O$ axis. (Ref. 4).

(c) If $S_1 \doteqdot S_2$ the damage relation follows the straight line $D = R$ and there is excellent agreement with the linear rule of damage accumulation.

The stress level S_2, in most works, lies in Region (2) which is fortuitous, as will be seen later, but quite understandable as this is the region of most clearly-defined endurances.

Evidence from Statistical Behaviour

Weibull in Ref. 19 has shown how the statistical distribution of S-N test points cycle-wise changes with stress level

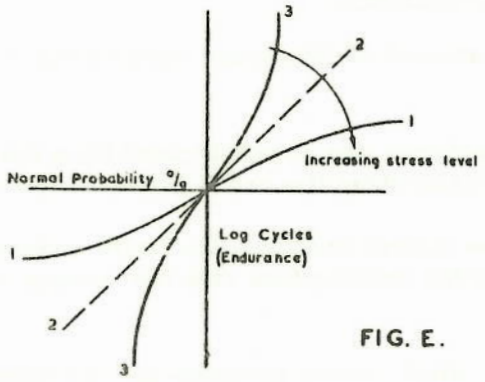

FIG. E.

(a) The curve (1) is seen to deviate from normal distribution in a manner suggesting that the distribution is being affected in the low probability of failure region so as to result in a distribution skewed thus:

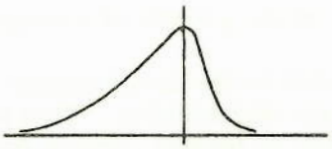

FIG. F.

(b) Curve (2), almost linear, represents the intermediate stress levels and presents an ideal normal population in most cases.

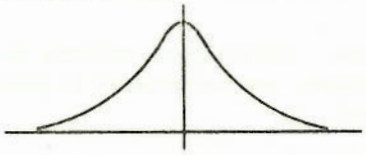

FIG. G.

(c) Curve (3) deviates due to effects in the high failure probability region, resulting in a distribution skewed, and then truncated at stresses near the so-called endurance limit.

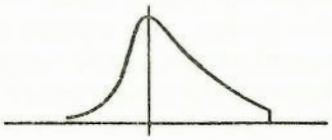

FIG. H.

In line with the current two-region "inflection point" concept, Weibull states,

> "The test points may follow a straight line rather closely with some specific very narrow range of test level, giving the impression of log-normal distribution. It is however impossible to fit the same distribution to data from significantly different test levels".

The statistical study thus emphasizes the complementary nature of the processes in regions (1) and (3). Rather than replacing the fundamental process exhibited in region (2), the secondary processes merely act in addition and finally swamp the fundamental process altogether at extreme values of stress.

Evidence from Physical Behaviour

A survey of a large amount of literature reveals the following interesting division of physical phenomena.

(a) High stress level fractures are characterized by a multiplicity of crack nuclei, i.e. something is accelerating the crack initiation process.

(b) Intermediate (and low stress levels in the finite endurance range) fatigue fractures are characterized by the propagation of a few cracks and general crack initiation is unaccelerated.

(c) Below the endurance limit, crack propagation has been wholly counterbalanced by some mechanism, but there is firm evidence that fatigue processes are still at work in this region as shown by their contributory effects on finite endurances. Perhaps the process of crack initiation still exists.

The Crack Initiation Process

There are two distinct phases in the growth of a fatigue crack. They are:

1. The crack initiation phase, - this is the development of a microcrack; i.e. the growth of a crack of microscopic dimensions. This phase has been proved to exist from almost the first cycle of fatigue, and in most types of fatigue test, it prevails for about 95% of the endurance. This stage is apparently completed when the crack assumes visual dimensions.

2. The crack propagation period. This phase covers the microscopic growth of the crack past the 'localized' phase, as its growth is now governed by the effect of its presence on the structure.

Constant-load testing of small non-redundant elements greatly accelerates this second phase, as has been pointed out by Weibull in Ref. 20. In fact, visual observations by the author during the tests currently made with plain specimens has shown that at intermediate or high stress levels, the second phase can be neglected in conventional testing. The attainment of the crack length corresponding to the completion of the first phase may then be taken as the criterion of failure in these cases. This is the most important assumption in the development of the crack theory for region (2).

In this section, the first phase is called 'crack growth', while crack propagation will only refer to the second phase. While the first phase is considered to be of fundamental importance in cumulative damage theory, the second is of tremendous practical importance in aircraft structures, for redundant structures of large cross-sectional area fail under the action of crack propagation. Ref. 21 emphasizes, however, the distinction which must be made between the two phases.

Because of the overshadowing economical importance of its brother, crack initiation has received very little attention, even though it is probably the key to

damage accumulation. If this is true, it can be readily seen how the second stage would tend to obscure any study of cumulative damage on composite structures.

Possible Crack Growth Relations

In 1946, J. A. Bennett obtained measurements of crack growth as given by the arc length of a microcrack on a specimen under rotating bending fatigue, using a stroboscope and a graduated-lens microscope. From this he obtained the relation (Ref. 8).

$$\log (L - C) = \gamma N \tag{5}$$

$$\text{i.e.} \quad h = Ae^{\gamma N} \tag{6}$$

where L is the circumferential length of the crack; C and γ are constants, being dependent on the stress.

This then gives the equation, from experiment, for crack growth. Its exponential nature satisfies all the fundamental characteristics, for these microcracks have often been reported to:

(a) exist from a very early point in the life of the specimen

(b) to grow exceedingly slowly for a very long period, and

(c) then to rapidly grow at a rate which seems to increase with the depth of crack attained.

If the attainment of a crack depth of a certain magnitude h_o is equivalent to failure, the relation then becomes

$$h_o = Ae^{\gamma N} \tag{7}$$

$$\text{or} \quad \log h_o = \log A + \gamma N$$

$$\gamma N = \log h_o - \log A = K_1 \text{, a constant}$$

$$\text{and} \quad \gamma = \frac{K_1}{N} \tag{8}$$

This term γ is the only parameter dependent on stress according to Ref. 8 and 3. Therefore its form is of fundamental importance in the development of a cumulative damage relation between stress levels.

A Power Function as the Parameter of Stress

To obtain a function to describe this stress parameter, Professor Shanley in Ref. 3 considers that the relation is connected in some way with plastic behaviour in a static tensile test. A power function has been derived to fit the plastic strain part

of this curve for aluminium. This was done by W. Ramberg and W. R. Osgood in describing stress-strain curves by three parameters. (Ref. 22). Shanley took this function in its general form for the parameter

$$\gamma = cs^x \tag{9}$$

where x is obtained from the stress-strain curve, fitting in the plastic range.

Thus $$s^x = \frac{K_2}{N} \tag{10}$$

which is a linear relation on log-log paper. It should be added that this expression also follows for a fatigue equation based on a constant rate of crack growth:

$$h_o = As^x N \tag{11}$$

which is certainly not characteristic of crack growth. Shanley then applied this to the whole of the S-N relation without regard to any corrections at different stress levels.

An Exponential Function as the Stress Parameter

The stress parameter is probably intimately connected with crystal behaviour in the plastic stress range. This behaviour is thought by the author to be slightly different in some way from conventional behaviour under static loading. Perhaps the static plastic behaviour considered by Professor Shanley is that for aggregate components, and not the same for single crystals acting as part of the aggregate.

If the degree of yeilding in the plastic range is not simply given by the particular conditions at the time, but is also governed by the previous strain history, it may be that this general mode of action, i.e. progress according to prior effect, is sufficient to describe the behaviour. Mathematical formulation of this particular property is given by:

$$\frac{d\gamma}{ds} = c\gamma \tag{12}$$

This states that the plastic state parameter changes with stress at a rate proportional to its prior magnitude. Solving:

$$\gamma = ke^{cs} \tag{13}$$

When substituted in (8)

$$e^{cs} = \frac{K_3}{N} \tag{14}$$

Thus: $$s = K_4 - \frac{1}{c} \log N \tag{15}$$

This is the equation of a straight line on a plot of stress versus log cycles.

E. S. Machlin (Ref. 23) developed the dislocation theory of physical metallurgy to account for the behaviour of "submicroscopic" cracks formed by fatigue. He proved that fatigue failure depends on plastic deformation, showed how multiplicity of crack initiation accounts for the brittle-like failure of metals in fatigue, and developed a comprehensive relation linking endurance with stress level, temperature, frequency, and material parameters. From this equation, the relation between stress and log cycles with other parameters fixed, is also linear in form.

Conversion to the Linear Rule

The final form of equation (6) is:

$$h = Ae^{e^{cs}n} \tag{16}$$

or for an arbitrary crack length denoting failure,

$$h_o = Ae^{e^{cs}N} \tag{17}$$

Combining (16) and (17)

$$\frac{h}{h_o} = e^{e^{cs}(n-N)} \tag{18}$$

Substituting equation (17) on the right side of this equation

$$\frac{h}{h_o} = \left(\frac{h_o}{A}\right)^{\frac{n}{N} - 1} \tag{18a}$$

Plotting these relations on a scale of crack depth versus cycle ratio, the curves will all have the same shape, i.e. the crack growth curves for different stress levels are affine. This simple characteristic means that the relation will follow the linear rule from one level of stress to another.

4. Load Spectrum

Before a simplified expression for the linear rule can be derived, it is necessary to consider the load spectrum.

The trans-Atlantic airliner project described in Ref. 24 is taken as an example, only the atmospheric gust spectrum being considered here, mainly because it is usually the most significant contributor to 'dangerous' fatigue damage. In addition the following data are also relevant:

Average passenger load factor	80%
Average fuel load at mid-flight	40%
Assumed cruising height	30,000 ft.
Approx. weight at mid-flight	240,000 lb.
Design service life	30,000 hrs.
Cruising speed (0.8 Mach)	543 mph T.A.S.
Total miles travelled (based on 500 mph)	15,000,000 miles
At 30,000 ft:	
Wing lift slope	4.77 per degree
Speed of sound	995 ft./sec.
$\sigma^{\frac{1}{2}}$	0.612

Gust Response. A satisfactory estimate of nominal gust response can be made using Airworthiness Requirements (B.C.A.R.) as described in Ref. 25. Equation 26 of this reference was used to obtain the loading due to a sharp-edged gust, taking into account tailplane and elevator effects. Using Fig. 5 of Ref. 24 (variation of lift curve slopes of surfaces and controls with Mach number) compressibility effects were also included. In the requirements for civil aircraft the static design gust velocity, 50 ft./sec. E.A.S. at 25,000 ft. drops linearly to 46 ft./sec. at the cruising altitude of 30,000 ft. This gust velocity was used to obtain the variation in response with altitude and weight and the resulting curves appear in Fig. 1.

Frequency of Occurrence. It has generally been found (Ref. 26) that:

(a) The relative frequency of gusts is essentially constant regardless of speed, altitude, or aircraft characteristics.

(b) The absolute frequency varies markedly with altitude, but is insensitive to speed of flight. For a given height, therefore, the absolute frequency, given by miles per gust, is largely independent of the aircraft. This is confirmed in Ref. 27.

Because of these points, it is possible to use the invaluable gust data based on Comet operations. The speeds, powerplant and altitudes for the projected jet airliner make the Comet data the only logical source for this analysis.

The Climb and Descent. For the Comet, Fig. 2 from Ref. 28 gives the variation in gust intensity with height in the climb and descent. The gusts per 1,000 miles greater than or equal to 10 ft./sec. have been plotted. The absolute frequency of gusts is seen

to vary enormously with height. Assuming that a gust gives the same final damage regardless of height, the effective fatigue height for climb and descent is:

$$H_F = \frac{\int_0^{30,000} (\text{gusts at height } h)\, dh}{\text{Gusts at sea level}}$$

Fig. 3 shows that the number of gusts greater or equal to 10 ft./sec. E.A.S. at sea level is 1,000 in 1,000 miles. By graphical integration and using the above relation:

$$H_F = 3,000 \text{ feet}$$

In this work the height is taken above sea level which is appropriate to trans-Atlantic service. Routes over ground require careful study as there is much evidence that gust intensity is governed by height above ground. Also the terrain has a marked effect on absolute frequency, especially at low or moderate altitudes.

The Effective Fatigue Height. To obtain the overall effective fatigue height, the gust intensities are weighted according to the time spent in each condition of flight. Assuming 10% of the time is spent in climb and descent and 90% of the time is spent at cruising altitude:

$$G_{H_F} = 0.9\, G_{cruise} + 0.1\, G_{climb}$$

where G_{H_F} = overall gusts per 1,000 miles at effective fatigue height.

G_{cruise} = gusts per 1,000 miles $\geq$ 10 ft./sec. at 30,000 ft. = 2.8

G_{climb} = gusts per 1,000 miles $\geq$ 10 ft./sec. at 3,000 ft. = 208

from Fig. 2.

Therefore $G_{H_F} = 0.9 \times 2.8 + 0.1 \times 208$

= 23.32 gusts $\geq$ 10 ft./sec. E.A.S. per 1,000 miles

= 425 miles per gust $\geq$ 10 ft./sec. E.A.S. From Fig. 2 this corresponds to

H_F = 12,000 ft.

Knowing the relative frequency of occurrence of gusts of different magnitudes, which is considered to be invariant with altitude (Ref. R.Ae.S. Data Sheet L.01.01), the number of miles per gust exceeding other values of E.A.S. can be determined. The line through these points, shown in Fig. 4, is then the required gust spectrum.

It is seen that the line coincides with the 5,200 ft. spectrum and not with the position which would be obtained by direct interpolation in the altitude variation of the relative frequency curves. This is because the gust intensity curve of climb and descent is significantly different from the one obtained from data on piston engined aircraft, which is used to show the altitude effect in Fig. 4.

The final gust load spectrum has thus been obtained and is shown in Fig. 4. It is thus evaluated in terms of distance which is the fundamental unit in gust research ("gust encountered" is a direct function of the distance covered).

Ref. 29 points out the danger of separating the relative frequency of gusts from the total number of gusts, as has been done in Ref. 30. Ref. 29 says "in doing this with data with widely different 'thresholds' below which no data are available, assumptions have to be made" in this respect. In the linear method of life assessment, the threshold is probably the most important single factor in the calculation. The use of 'miles per gust' overcomes the problem as it combines relative frequency with absolute frequency.

In tabulating this spectrum in Table 1, use is made of the linear extrapolation to U = 0 ft./sec. gust velocity to determine the intercept value log N_o. This is standard procedure in Swedish work, and is implicit in many other reports, e.g. the region near the lg line is for "reasons inherent in the technique of measurement never very accurately ascertainable. However, for practical requirements it should be sufficiently well defined by linear extrapolation". (Dr. Gassner in Ref. 6).

Certain aircraft parameters, such as centre of gravity position, short-period damping and wing bending flexibility all tend to give a wide variation in response throughout the structure. (Refs. 31, 32). Therefore, the incremental load factor varies with a given gust velocity due to variations in response. The stress level also varies with a given load factor due to eccentricity of loading, distance of the detail from the neutral axis of the component and the area of material used.

Perhaps the best method of dealing with these two variations, is to set up an envelope load spectrum covering all the probable response cases. Fig. 1 shows that the worst value for the nominal load factor increment is about 2.5. This value should then cater for the weight, aeroelastic load amplification and the other factors affecting response. The final level chosen should be checked with the maximum static limit load factor which is usually of the same order of magnitude. $n = 1 + 2.5 = 3.5$ which occurs once in ten years (Ref. 33.). $n_{limit} = 3.6$ for the aircraft wing.

Gust Spectrum Theory. Dr. Gassner, in Ref. 6, has stated that the load spectrum follows a logarithmic binomial distribution. He has obtained good agreement with the empirical data accumulated by Taylor (Refs. 27, 32). These experimental results have been represented by a linear plot of the gust frequency on semilogarithmic paper in common with many other data from the other centres of research.

The equation of a straight line is given by

$$n = n_o^{\,1 - \frac{y}{y_m}}$$

where y is a function of the gust velocity.

This equation is then the equation of the gust summation curve, thus for any quantity y there is a value log N which represents the total number of the quantity of y above and at that level. It is therefore an integration curve for all values taken from the maximum, y_m.

The decision as to what value y_m should take depends on considerations of integration of the load spectrum with static requirements, i.e. the value of y_m to settle upon becomes restricted when it is related to the material properties, for the minimum rational value of Log N is that corresponding to $\frac{1}{4}$ cycle. This can be called the Static Axis, for all static failures represent the completion of $\frac{1}{4}$ cycle of fatigue.

A dove-tailing of static and fatigue loads is quite possible here, for the static gust cases have evolved through the years due to the frequency of occurrence of these gusts. It is not surprising, therefore, that the spectrum ties in closely with the single occurrence of a gust at about the limit load (actually 49 ft./sec. when extrapolated) in the 30,000 hour life chosen.

In the assessment of aircraft life, the cycle ratio appears to be a fundamental unit. Because of this, it is necessary to determine not the sum of all cycles at and above the given level, but only the number of cycles at the particular level.

Since the summation is a continuous curve, the required number of cycles is obtained from a differentiation of the summation equation thus:

$$\frac{dn}{dy} = \frac{d(N_o^{\,1 - y/y_m})}{d(1 - y/y_m)} \cdot \frac{d(1 - y/y_m)}{dy}$$

$$= N_o^{\,1 - y/y_m} \cdot \log_e N_o \cdot \frac{1}{y_m}$$

$$= \frac{\log_e N_o}{y_m} \cdot n \cdot$$

summation

The exponential differentiation results in a factor on the original equation. Thus the differentiated spectrum is a straight line parallel to the summation line. Its intercept on the y = 0 axis is:

$$(N_o)\ \text{differentiated} = N_{o_d} = \frac{\log_e N_o}{y_{m_s}} \cdot N_{o_{summation}}$$

In the summation curve of Fig. 4 used to draw up Table 1:

$$N_o = 8{,}340{,}000$$

$$\log_e N_o = 15.91$$

Then $$\frac{\log_e N_o}{y_{m_{summation}}} = \frac{15.91}{49}, \quad \text{if } y_{m_s} = (U_{max})_{\substack{\text{zero} \\ \log \text{ axis}}} = 49 \text{ ft./sec.}$$

$$= 0.325$$

Therefore $$N_{o_d} = 0.325\ N_{o_s} = 0.325 \times 8{,}340{,}000$$

$$= 2{,}720{,}000 \text{ cycles.}$$

Thus a line parallel to the summation line, but beginning at 2,720,000 cycles at the U = 0 axis represents the spectrum in unit gust velocity intervals. Table 1 when plotted gives the same line but less accurately. It involves the tedious process, common in this work, of taking differences from the summation curve.

The quantity y is intentionally made a general function in order to avoid certain pitfalls in the use of gust spectra. It is defined by the equation $y = f(U)$ where U is gust velocity. If y is used to denote stress, it is assumed to be a linear function of the gust velocity.

For agiven stress level, the cycle ratio is the quantity of interest, and a general expression for it follows. The cycle ratio depends on:

(a) The interval of differentiation: $N_{o_d} = \frac{\log_e N_{o_s}}{y_{m_s}} \cdot N_{o_s}^{(1 - y/y_{m_s})}$

(b) The stress-gust velocity relation: $n_d = N_{o_d}^{(1 - y/y_{m_d})}$

Thus $$n = \left[\frac{\log_e N_{o_s}}{y_{m_s}} \cdot N_{o_s}^{(1 - y/y_{m_s})} \right]^{(1 - y/y_{m_d})}$$

Because of the two factors (a) and (b), the final expression for the cycle number n_d is the quadratic:

$$\log_{10} n_d = (A - By)\left(1 - y/y_{m_d}\right)$$

where $$A = \log_{10}\left(\frac{\log_e N_{o_s}}{y_{m_s}}\right) + \log_{10} N_{o_s}$$

and $$A = \log_{10} \frac{N_{o_s}}{y_{m_s}}$$

A and B are then fixed once the summation curve has been chosen. The simple summation afforded by using unit intervals of gust velocity in the differentiation is a strong argument for its use. This would standardize the present position where intervals of 0.1, 0.5, and even 3.0 fps (4.5 fps - Ref. 30) have been taken without explanation. What happens when these different intervals are taken is shown below:

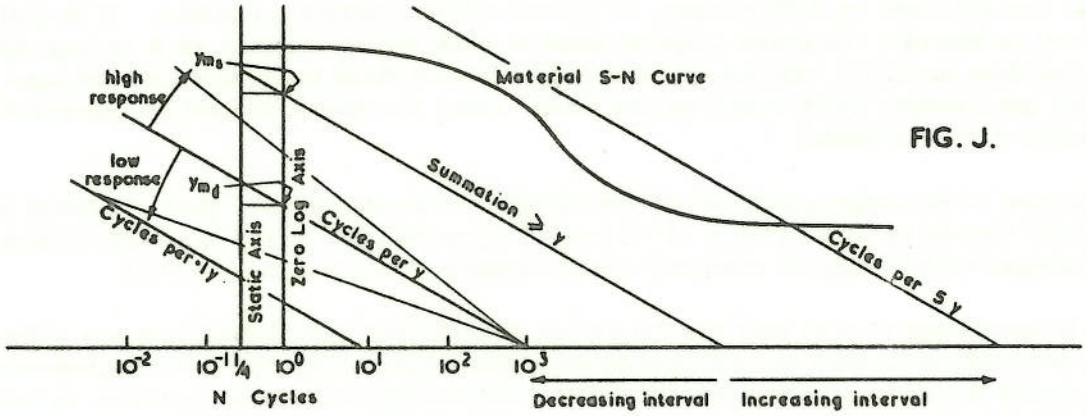

FIG. J.

The Take-Off and Landing Cycle. For the project aircraft, (Ref. 24) it has been conservatively assumed that 1,000 flights are made each year.

By arbitrarily defining the mid-cruise bending moment as the datum (i.e. the lg level of stress) the effective stress levels are:

(1) Mid cruise: lg for 2.496×10^6 lb.ft.

(2) Pre take-off: $-\frac{2.730}{2.496} = -1.09$ g due to weight of fuel.

(3) Post take-off: $\frac{1.877}{2.496}$ = 0.75 g due to fuel relief.

(4) Pre landing: $\frac{2.206}{2.496}$ = 0.88 g due to low weight.

(5) Post landing: $-\frac{0.797}{2.496}$ = - 0.32 g due to wing weight alone.

These results are plotted graphically in Fig. 5. The wing has a "cycle" of $\pm$ 1g about mean stress from this periodic change in loads.

Ref. 27 states that 99% of all gust peaks away from level flight (1g) return to 1g before moving away again. This statement does not refer to all the gust peaks on the trace but to a smoothed out substitute trace, where all changes of 0.1g or less have been ignored. A cycle of fatigue is defined as one positive gust and one negative gust of equal magnitude.

The spectrum finally used can be in the form of a bar chart where the gusts per interval are obtained by differences, or by the differentiation technique. It is quite important to indicate the class interval used in such differentiation as it is impossible to use the data properly without the knowledge for the final integration of damage. If one uses the Swedish work based on the linear rule, the usual method of numerical integration can be avoided.

The use of envelope spectrum is definitely recommended, for gust response or sensitivity varies so much that it is virtually impossible to cater for every change in the response while trying to consider the frequency of occurrence as well.

It is important to note that the American and British gust definitions are different, but the alleviation factors are defined in different ways so that the two requirements are virtually the same. However without the alleviating factors the relation in units between the two definitions in gust velocity is given by $U_{Amer.} = 0.6U_{British}$.

The following table is taken from Fig. 4.

U fps	Cycles from the Envelope Spectrum: Miles per cycle ≥ U (i.e. 1 + & 1 - gust)	Cycles per 15 million miles ≥ U
0	1.8	8,340,000
2.5	4	3,750,000
5	9	1,665,000
10	44	341,000
15	230	65,300
20	1,000	15,000
25	5,000	3,000
30	28,000	535
35	140,000	107
40	780,000	30
45	4,000,000	3.75
50	20,000,000	0.75

5. Simplification of the Linear Rule

This section will derive a simplified expression for the linear rule where the load spectrum and the corresponding material S-N relation may be represented by two straight lines on a semilog plot. The S-N relation is here shown in terms of the equivalent gust velocity.

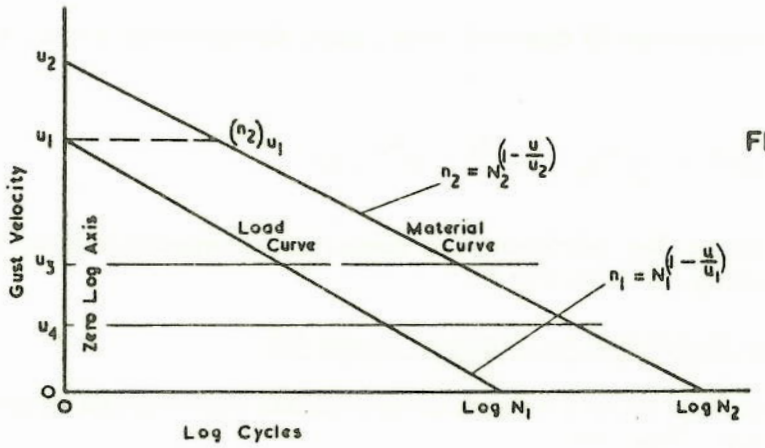

FIG.K.

The general equation of a straight line given by its axes intercepts is:

$$n = N^{\left(1-\frac{u}{u_{max}}\right)} \qquad (19)$$

The general expression for the cycle ratio is:

$$\frac{n_1}{n_2} = \frac{N_1^{(1 - \frac{u}{u_1})}}{N_2^{(1 - \frac{u}{u_2})}} = \frac{N_1}{N_2}\left(\frac{N_2^{\frac{1}{u_2}}}{N_1^{\frac{1}{u_1}}}\right)^u \tag{20}$$

Often u_2 is difficult to obtain directly. Its value can be obtained from the value n_2 at the level of u_1, i.e.

$$u_2 = \frac{u_1}{\frac{(\log n_2)}{\log N_2} u_1} \tag{21}$$

Let 'a' represent the constant $\frac{N_1}{N_2}$ and let 'r' represent the constant in the brackets in equation (20). Thus the cycle ratio $R = ar^u$. This shows that cycle ratios merely form a geometric progression. If the interval of gust velocity taken is unit feet per second, the linear rule is simply the sum of this procession, i.e.

$$\sum_{u=0}^{u_1} ar^u = \frac{a(r^{u_1} - 1)}{r - 1} \tag{22}$$

If the linear rule summation is desired over, say, the interval $u = u_3$ to $u = u_4$ the expression is:

$$\sum_{u_4}^{u_3} ar^u = \frac{a}{r - 1}\left(r^{u_3} - r^{u_4} - 1\right) \tag{23}$$

This simple expression then performs the numerical integration of cycle ratios for the ideal process following the linear rule.

Cumulative Damage Behaviour in Regions (1) and (3)

Two sources of data were available to assess the corrections necessary in these areas of nonlinearity. They are:

(a) The 0.5 Probability S-N curve of endurance with the plain specimens tested as indicated in the appendices, shown in Fig. 5 and

(b) The results of the partial damage tests carried out with the same specimen type described in Appendix I, and shown in Table 2. The general layout of these tests is also shown in Fig. 6.

In order to correlate at least qualitatively the results from both of these sources, the curve of the S-N relation was rotated, to present the straight line portion of Region (2) as a region of constant damage activity. No attempt is made to define this activity, it is merely used to form a qualitative starting point. The result appears in Fig. 7.

Once this has been done, the boundaries of each region were decided and drawn as shown. Then the results of the reduction of the partial damage data given in Table 2 were superimposed.

From the partial damage results in Region (1) the acceleration of the fundamental process is quite evident, as the relation appears to be approximately:

$$D = R^{1/10} \tag{24}$$

The limiting case for Region (1), given by the static test results, can be represented by the equation:

$$D = R^{0} \tag{25}$$

When the static results are considered together with the fatigue results, the non-linear S-N curve in Region (1) suggests the relation:

$$D = R^{x} \tag{26}$$

where x moves from unity in Region (2) to 0.1 in the area of the partial damage tests to zero at the static axis. The total damage for Region (1) in the example has been evaluated and is shown in Table 2.

In Region (2), the results indicate that the damage was so small from the first level as to not survive the effects of scatter; i.e. the mean endurance at the second level fell within the confidence limits of the mean of the endurance from single level testing, as shown in Fig. 8. This seems unfortunate, but in view of the significant results obtained in Region (1), it is obvious that the damage function must be close to being linear in this region, for the cycle ratios used are less than one per cent. They therefore could cause comparatively little damage if the linear rule were valid here. For the example:

$$N_1 = N_2 = N \doteq 3{,}000{,}000 \text{ cycles (Fig. 6)}$$

Thus $a = 1$

$u_1 = 42$ ft./sec.

$u_2 = 96$ ft./sec.

Hence $r = N^{\left(\frac{1}{u_2} - \frac{1}{u_1}\right)} = N^{-0.014} = 0.844$

Summing from equation (22)

$$\sum_{o}^{42} ar^{u} = \frac{1 - r^{42}}{1 - r} = \frac{0.990}{0.156} = 6.35 \qquad (27)$$

In Region (3) the partial damage test data indicated that healing was encountered at the lower levels. The behaviour in this region suggests the relation:

$$D = R - R^{y} \qquad (28)$$

i.e. the fundamental process is being balanced by a function dependent on stress level and cycle ratio. In the limiting case, u = 0, no damage could be possible.

$$\text{i.e.} \quad D = R - R^{1} = 0 \qquad (29)$$

The healing function seems to prevent actual propagation, and is responsible for the endurance limit effect. At the lowest level of the partial damage tests,

$$D = R - R^{y} = -0.60 \text{ from Table 2.}$$

If the linear rule prevailed as in Region (2)

$$D = R = 0.37$$

Thus the healing function at this level is

$$R^{y} = 0.60 + 0.37 = 1.0$$

Thus x = 0 in this region.

From the results at the other two levels in Region (3), the healing function rapidly dies away some distance below the endurance limit stress. These restrictions on the healing function led the author to the following form:

$$R^{y} = R^{(\frac{u}{u_H} - 1)^2} \qquad (30)$$

where u_H is a level of maximum healing action. This function satisfies all the restrictions above, and the summation for the example is given in Table 2.

The Final Form of the Corrected Rule

In its corrected form the rule states that failure will occur when,

$$D_1 + D_2 + D_3 = 1$$

$$\text{i.e.} \quad \Sigma R^{x} + \Sigma R + \Sigma R^{(\frac{u}{u_H} - 1)^2} = 1 \qquad (31)$$

In the example,

$$\sum_{43}^{48} R^{0.1} + \sum_{o}^{42} R - \sum_{o}^{10} R^{\left(\frac{u}{5} - 1\right)^2} = 2.765 + 6.350 - 8.555$$

$$= 0.56$$

The summation of damage states that 56% of the life has been used up. The actual life of the element based on the 30,000 hours load spectrum is then 53,500 hours.

While this corrected form requires more than just the simple S-N curve and the appropriate spectrum, further work on the correlation between two level tests and S-N non-linearity may ultimately allow such simplification, merely by carefully constructing the S-N relation. The method will then be as quick and almost as simple as the present basic linear rule. It may then be extended so that correction parameters may be evaluated for practical aircraft materials relative to some basic load spectrum.

The damage curve for using the uncorrected linear rule on the spectrum and S-N curve of the example is shown in Fig. 9. The total damage by this method was 0.235, i.e. 23,5% of the life was used up. This would give an uncorrected lifetime of 128,000 hours. The damage curve using the corrected rule is shown in Fig. 10. The partial damage results have been superimposed. The general forms of the non-linear components in Equation 31 are shown to follow the experimental results faithfully.

Conclusions

1. The non-linear effects as evaluated in the example each appear to be of the same order as the basic linear damage. They thus represent good examples of the significance of non-linear damage accumulation. Part of the severity of Region (1) may be a direct result of the use of a precipitation-treated aluminium alloy.

   Regardless of the particular results of this data, the general method of performing a 'partial damage traverse' of the stress levels met in service is suggested as a good procedure to gauge damage activity qualitatively. Comparison with data of other research works was not possible, as the particular conditions of material, mode of testing, mean stress, statistical accuracy and machine scatter factor have not been found in agreement with the present work.

2. Much work should be done to study the characteristics of crack initiation and the transition to the process of crack propagation. Little is really known about this part of crack growth. It would be of great use to know whether the assumption of affine crack growth with stress can be relied upon for the ideal fatigue process.

3. It is unfortunate that the principles developed in this method cannot be readily put to a test which exactly simulates service conditions, and is governed by the same spectrum of loads. Such a random load test would quickly prove the worth of any cumulative damage theory. Until such tests are possible, more

sophisticated sequence programmes for loading are not of any more value than the two-level testing procedure used here, as all these arbitrary modes of testing will probably require their own particular corrections for random loading.

4. Many workers in this field have turned to non-affine crack growth equations and other difficult relations in their efforts to obtain one relation which will fit the overall picture. This is the important point on which the present work differs. The chief difference between the procedure proposed here, and the work of other research centres lies not in fundamental formulation, but in its application.

While the continuing lack of success of these other theories does not mean that they are less promising in comparison, the evidence given here seems to show that practical use can be made of this new method. From the substantial degree of success the basic linear rule has had in the past, the author is convinced that only a procedure fundamentally based on it will have any measure of success in practical engineering.

6. References

1. MINER, M. — Cumulative Damage in Fatigue. Jnl. Applied Mechanics, September, 1945.

2. SCHIJVE, J., JACOBS, F. — Fatigue Tests in Notched and Unnotched Clad 24.S.T. Sheet Specimens to Verify the Cumulative Damage Hypothesis. N.L.L. Report M.1982, April, 1955.

3. SHANLEY, F.R. — A Theory of Fatigue Based on Unbonding during Reversed Slip. Rand Publication P.350, May. 1953.

4. — The Fatigue of Metals and Structures. Navaer 00 - 25-53, U.S. Government Printing Office, 1954.

5. HEYWOOD, R.B. — The Influence of Preloading on the Fatigue Life of Aircraft Components and Structures. R.A.E. Report Structures 182.

6. GASSNER, E. — The Problem of Fatigue Strength in Aircraft Structures. Translated by T. Haas, Aircraft Engineering, July, 1956.

7. WALLGREEN, G. — Fatigue Tests with Stress Cycles of Varying Amplitude. F.F.A. Report 28.

8. BENNETT, J.A. — A Study of the Damaging Effect of Fatigue Stressing on X4130 Steel. A.S.T.M. Proceedings, 1946.

9. NEWMARK, N.M. — A Review of Cumulative Damage in Fatigue, in "Fatigue and Fracture of Metals", edited by W.M.Murray. Wiley, 1952.

10. MARCO and STARKEY — A Concept of Fatigue Damage. Trans. A.S.M.E. 76, 1954.

11. WILKINS, E.W.C. — Cumulative Damage in Fatigue. International Colloquium on Fatigue, Stockholm, 1955.

12. LEVY, J.C. — Cumulative Damage in Fatigue - A Design Method based on the S-N Curve. J.R.Ae.S., July, 1957.

References (Continued)

13.	HENREY, D.L.	A Theory of Fatigue Damage Accumulation in Steel. Trans. A.S.M.E., vol.77, August, 1955.
14.	SCHIJVE, J., JACOBS, F.A.	Research on Cumulative Damage in the Fatigue of Riveted Aluminium Alloy Joints. N.L.L. Report M.1999.
15.	MILES, J.W.	On Structural Fatigue under Random Loading. Jnl. Aero. Scs., November, 1954.
16.	FREUDENTHAL, A.M.	Physical and Statistical Aspects of Cumulative Damage. Stockholm Colloquium on Fatigue, May, 1955.
17.	WEIBULL, W.	A New Method for the Statistical Treatment of Fatigue Data. SAAB T.N.30, May, 1954.
18.	LUNDBERG, B.	Fatigue Life of Aircraft Structures. F.F.A. Report 60.
19.	WEIBULL, W.	The Scatter of Fatigue Life and Fatigue Strength of Aircraft Structural Materials and Parts. F.F.A. Report 73, November, 1956.
20.	WEIBULL, W.	Effect of Crack Length and Stress Amplitude on the Growth of Fatigue Cracks. F.F.A. Report 65, May, 1956.
21.	BENNETT, J.A.	The Distinction between Initiation and Propagation of a Fatigue Crack. Session 6, Proceedings of the International Conference on Fatigue of Metals, 1956.
22.	RAMBERG, W., OSGOOD, W.R.	Description of Stress-Strain Curves by Three Parameters. N.A.C.A. Tech.Note No. 902, July, 1943.
23.	MACHLIN, E.S.	Dislocation Theory of the Fatigue of Metals. N.A.C.A. Tech. Note No. 1489.
24.		1957 Project - Trans-Atlantic Airliner. Design Note Des/65, Department of Aircraft Design, The College of Aeronautics.

References (Continued)

25.		Requirements, Loading and Stressing Cases (B.C.A.R.). Lecture Supplement Des/42, Department of Aircraft Design, The College of Aeronautics.
26.	TYE, W.	The Outlook on Airframe Fatigue. J.R.Ae.S., May, 1953.
27.	TAYLOR, J.	Measurement of Gust Loads in Aircraft. J.R.Ae.S., February, 1953.
28.	TAYLOR, J.	Fatigue Loads and their Effect on Aircraft Structures. Appendix 1, Third Conference of the International Committee on Aeronautical Fatigue, Cranfield, January, 1955.
29.	KLOOS, J.	Gust Loads, Appendix 8, Second Conference of the International Committee on Aeronautical Fatigue, Stockholm, 1953.
30.	RHODE, R.V., DONELY, P.	Frequency of Occurrence of Atmospheric Gusts and of Related Loads on Airplane Structures. N.A.C.A., A.R.R. L.4121, 1944.
31.	PRESS, H., HOUBOLT, J.C.	Applying Generalized Harmonic Analysis to Aircraft Gust Loads. Jnl. Aero. Scs. January, 1955.
32.	TAYLOR, J.	Gusts and their Measurement. J.R.Ae.S., December, 1954.
33.	CHEVERTON, H.	The Effect of Fatigue on Aircraft Design. External Design Lecture, February, 1958, The College of Aeronautics.
34.	WEIBULL, W.	Scatter in Fatigue Tests. Minutes of the Second Conference of the International Committee on Aeronautical Fatigue. Appendix 2, September, 1953.
35.	RANSOM, J.T.	Discussion by W. Weibull, Statistical Methods for Fatigue. Colloquium on Fatigue, May 1955, p.232.

References (Continued)

36.	WEIBULL, W.	Static Strength and Fatigue Properties of Unnotched Circular 75 S-T Specimen under Repeated Tension. F.F.A. Report 68, June, 1956.
37.	WEIBULL, W.	Statistical Handling of Fatigue Data and the Planning of Small Test Series. F.F.A. Report 69, October, 1956.
38.	BENDER, A., HAMM, A.	The Application of Probability Paper to Life on Fatigue Testing. Engineering Dept., Delco Remy, General Motors Corporation.

APPENDIX I

Experimental Test Data

The Test Programme

The machine used in these tests was the College of Aeronautics Design Department Losenhausen Pulsator, static tensile capacity 77,000 lb. and dynamic capacity 46,200 lb.

The fatigue specimen was machined from $1\frac{1}{2}$ in. diameter L.65 extruded bar stock to give a nominal diameter of 0.564" over the central portion. A high degree of repeatability was achieved by turning the specimens on a profile lathe using a case-hardened steel profile. The specimen is shown in Fig. 11.

The fillet used to bring the stress level to a maximum in the 2 in. centre parallel section is a plot of the trigonometric tangent function between $\pm$ 90 degrees. The fillet curve was chosen as it acts best as the envelope of the normals to the photo-elastic fringe lines in the bar (lines of constant difference in principal stress). Appendix III discusses a $\frac{1}{4}$ in. plate photoelastic model of the specimen under a tensile loading with this configuration.

In all, 156 specimens were machined along with two specimens made from L.40. The first L.40 piece was used to check the profile and the second was used to augment the calibration programme.

The utilization of specimens was as follows :

(a)	Derivation of the basic S-N curve: 8 levels at 9 each	72
(b)	The two-level partial damage tests: 8 levels at 9 each	72
(c)	The take-off and landing fatigue case:	5
(d)	Calibration of the fatigue machine:	5
(e)	Defectives:	4
	Total:	158

All specimens were tested in a random manner consistent with the most efficient use of time and availability of specimens.

The bar stock was received from a single melt of aluminium alloy made under the requirements of British Standard Specification L.65, for extruded bars of 1 to 4 in. in diameter.

As there was some question of end effects in the plastic region of the stress-strain curve (since the central portion was only 2 in. long) seven of the specimens were machined to give a continuation of $\frac{1}{4}$ in. at each end of the parallel section. The fillets were unchanged and were merely moved away from the centre thereby reducing

the clamping section by a small amount. Two tests were carried out with the normal configuration to compare behaviour. No appreciable difference was discernable, save for a slight tendency of the unaltered specimens to remain elastic for a slightly higher load. These results appear to lie satisfactorily within the scatter of the other results.

Specimen Hardness Tests

Using a Vickers Diamond Pyramid Hardness testing machine with 30 kg. load, discs of the L.65 material were tested for hardness at intervals of approximately ten specimens throughout the test programme. These discs were machined and faced from the discarded stock gripped by the chuck of the profile lathe.

It was decided to check the hardness of any specimens which gave abnormal fatigue results. No. 67 specimen failed at an abnormally low number of cycles. Two sections were taken, one in the fillet and one in the centre parallel portion after failure and checked for hardness. No other specimen was checked as the results showed a satisfactorily low value of scatter.

The hardness of the L.65 specimens ranged from VHP/30/150 to 169, with a mean hardness value of VHP/30/165. The hardness of No. 67 (neck) is 2% greater and the hardness of No. 67 (fillet) is only 1% greater than the mean. It is therefore, considered to have failed merely at an extremely low probability value with nevertheless is statistically possible. The scatter in hardness values was $\pm$ 2 to $\pm$ 3% at most. The hardness values are therefore satisfactory, and the melt was of a high standard of homogeneity.

STATIC CONTROL TESTS

Specimen No. -Diameter	0.1% Proof Stress p.s.i.	0.2% Proof Stress p.s.i.	Tensile Ultimate p.s.i.	Elastic Modulus p.s.i.	Elongation % 2 inches
*8 0.564"	73,000	73,300	80,900	10,590,000	11
22L 0.564"	72,700	74,250	80,500	10,150,000	12
33 0.564"	73,900	74,750	80,500	10,700,000	10
38L 0.563"	71,750	72,500	78,250	10,400,000	11.5
39L 0.564"	72,100	73,000	79,100	10,550,000	11
40L 0.564"	73,500	76,000	80,900	10,650,000	12
41L 0.564"	73,400	74,250	80,500	10,310,000	11
42L 0.565"	74,200	74,750	80,500	10,650,000	11
43L 0.565"	72,700	73,800	79,750	10,100,000	12

*This specimen photographed on fracture.

FATIGUE TEST RESULTS - Basic S-N Curve

Level A — Loading: 20,000 ± 47,000 psi

Specimen No.	Total Cycles
1	900
68	1350
69	2180
70	950
72	800
74	2810
75	1470
76	1920
77	1600

Level B Loading: 20,000 ± 42,000 psi

Specimen No.	Total Cycles
2	1450
11	5200
12	4550
13	10700
15	3950
21	4160
23	3440
24	3320
25	3430

Level C Loading: 20,000 ± 37,000 psi

Specimen No.	Total Cycles
7	12,560
26	4,950
27	13,280
29	8,550
30	9,000
31	10,960
34	13,780
35	7,880
37	11,600

Level D Loading: 20,000 ± 32,000 psi

Specimen No.	Total Cycles
6	21,780
44	35,800
45	21,660
54	27,160
55	45,810
63	44,080
64	31,830
65	32,660
66	32,390

Level E Loading: 20,000 $\pm$ 27,000 psi

Specimen No.	Total Cycles
5	35,520
46	40,380
47	53,780
52	68,100
59	37,450
60	68,270
61	65,320
62	88,810
71	84,550

Level F Loading: 20,000 ± 22,000 psi

Specimen No.	Total Cycles
9	111,660
32	265,420
48	175,000
49	119,960
50	211,610
53	259,800
56	133,010
57	233,850
73	117,420

Level G Loading: 20,000 ± 17,000 psi

Specimen No.	Total Cycles
3	700,930
14	1,318,300
17	853,860
18	2,413,620
19	3,354,550
20	767,770
51	3,302,660
58	969,650
67	287,120
36	1,593,710

FATIGUE TEST RESULTS - Special Case

Take-off and Landing

Loading: Zero $\pm$ 20,000 psi

Specimen No.	Total Cycles
152	1,562,850
153	1,162,700
154	1,731,950
155	4,453,000
156	1,664,870

FATIGUE TEST RESULTS - Partial Damage Tests

Loading: $\frac{1}{2}$ cycle (positive) of
20,000 ± 27,000 psi

Then Level E: 20,000 ± 27,000 psi

Specimen No.	Total Cycles at Level E
78	33,840
79	29,270
81	53,640
83	25,450
84	17,800
85	27,210
116	49,700
118	50,630
124	65,590

FATIGUE TEST RESULTS - Partial Damage Tests

Loading: 1 cycle of 20,000 $\pm$ 50,000 psi

Then Level E: 20,000 $\pm$ 27,000 psi

Specimen No.	Total Cycles at Level E
95	20,650
96	26,370
97	13,920
98	22,480
105	15,950
106	12,710
121	19,470
125	16,760
129	21,680

FATIGUE TEST RESULTS - Partial Damage Tests

Loading: $2\frac{1}{2}$ cycles of 20,000 $\pm$ 47,000 psi
(Level A)

Then Level E: 20,000 $\pm$ 27,000 psi

Specimen No.	Total Cycles at Level E
107	17,910
108	20,430
111	23,040
112	14,620
113	14,560
122	55,220
126	24,700
130	19,960
131	30,500

FATIGUE TEST RESULTS - Partial Damage Tests

Loading: 10 cycles of 20,000 ± 42,000 psi (Level B)

Then Level E: 20,000 ± 27,000 psi

Specimen No.	Total Cycles at Level E
80	48,720
82	72,240
114	51,840
115	64,920
117	42,320
120	68,550
123	70,040
127	47,190
128	57,780

FATIGUE TEST RESULTS - Partially Damage Tests

Loading: 43 cycles of 20,000 $\pm$ 37,000 psi (Level C) Manually

Then Level E: 20,000 $\pm$ 27,000 psi

Specimen No.	Total Cycles at Level E
94	51,280
99	72,860
109	55,730
119	82,370
132	67,270
133	49,760
134	49,060
138	95,640
141	64,670

FATIGUE TEST RESULTS - Partial Damage Tests

Loading: 15,000 cycles of 20,000 $\pm$ 17,000 psi (Level G) at 600 cpm

Then Level E: 20,000 $\pm$ 27,000 psi

Specimen No.	Total Cycles at Level E
88	49,610
93	56,350
102	85,200
103	61,580
104	71,540
110	91,380
135	65,750
136	68,770
137	53,180

FATIGUE TEST RESULTS - Partial Damage Tests

Loading: 72,000 cycles of 20,000 $\pm$ 12,000 psi (Level H) at 600 cpm

Then Level E: 20,000 $\pm$ 27,000 psi

Specimen No.	Total Cycles at Level E
86	42,730
87	57,770
91	83,780
92	56,640
101	71,150
140	91,770
144	61,500
150	44,450
151	64,750

FATIGUE TEST RESULTS - Partial Damage Tests

Loading: 370,000 cycles of 20,000 $\pm$ 7,000 psi (Level J) at 600 cpm

Then Level E: 20,000 $\pm$ 27,000 psi

Specimen No.	Total Cycles at Level E
89	71,350
142	77,790
143	124,320
100	102,100
145	75,070
146	99,310
147	90,780
149	84,910
148	106,580

APPENDIX II

The Statistical Treatment of Test Data

Statistical Notation

x Value of endurance obtained as part of a sample

$\bar{x}$ Mean value of endurance for a given sample

s Standard deviation of a sample = $\sqrt{\dfrac{\Sigma x^2 - \dfrac{(\Sigma x)^2}{n}}{n - 1}}$

n Number of tests in a sample

X Mean of the population of an infinite number of tests for the endurance at a given level

σ Population standard deviation

U Standard deviate of the population

u Standard deviate of the sample

P Probability of failure for the population

p Probability of failure of the sample.

Planning the Tests. Weibull, in Ref. 34, states that, assuming the normal distribution is satisfactory, the evaluation of scatter by the standard deviation requires 20 specimens for normal research accuracy. To determine which distribution of population is being followed, a further 100 at least are required.

In the tests carried out in conjunction with this study, the aspect of linearity in the S-N curve was to be investigated. If the test had been a simple S-N evaluation, Weibull was able to show that it is always better to use as few stress levels as possible rather than a number of levels, if the number of specimens is limited. However, this is restricted by the fact that the top level must be well below the "inflection point" of the S-N curve, and the lower level "well above the endurance limit" which diminishes the importance of this testing rule. If the testing time is at a premium, the highest statistical accuracy occurs if the levels and number of specimens in each are chosen on an equal time basis. This of course is a difficult thing to predict beforehand, and also complicates the statistical treatment of the results. For these reasons the testing was restricted to a uniform nine specimens regardless of load level.

The Concept of Confidence. It is usual to test as many specimens for a given case as is feasible - generally from 6 to 10. The statistical conclusions derived from the sample of test pieces will be 'uncertain' since these conclusions have assumed that the population from which the sample came had exactly the same general characteristics. Fortunately, the Concept of Confidence enables the experimenter to say, for instance, "there are nine chances in ten that this sample has characteristics identical to this population".

Assuming that the results are following a log-normal distribution, the Concept of Confidence will quantitatively ascertain the degree of uncertainty expressed. The mean and the standard deviation of each, sample and population, will give two scales of probability. Small sample statistics have created a coefficient k to apply to the sample standard deviations so that, for a given degree of confidence, such as 9 chances in 10, or 90%, the population probability, normally given by $\bar{X} - U\sigma$, will fall within the region $(\bar{x}, \bar{x} - ks)$. There is a 90% chance that the population probability lies ahead of the point $\bar{x} - ks$, and a 10% chance that it lies before this point. Figure 12, taken from Ref. 18, shows how this value varies with sample size. It is easy to see that an optimum number of test pieces for a practical test can be obtained avoiding very large values of k while at the same time not showing an increase in accuracy compatible with the cost of increased testing. If probabilities are required to be delineated to within 1%, instead of 10%, 99 tests are needed instead of 9. Similarly, 999 tests are required for a 0.1% probability scale.

Using nine specimens per level in the testing, the value of k for each probability was used to determine the limits for the population probabilities at the 90% confidence levels (which seems a reasonable level for fatigue results). The effect of this latitude or margin is shown on the normal probability curves, Figs. 13 - 21. The test results fall inside the margin in all cases.

In the figures the scatter is shown directly as differences in the logs; i.e. (log i - the log mean). The samples of results obtained in the tests for the evaluation of the S-N curve for L.65 bar have been presented on probability paper in Figs. 13 - 21. These results do not of course fall on the straight line which denotes the normal population for their standard deviation for three reasons:

(a) Population characteristics are not identical with the sample, as the sample characteristic relation is 'uncertain'.

(b) The population distribution may be affected by many different factors. During a test, machine variations induce an additional scatter of roughly the same order as the basic properties. If the material comes from two different melts, two populations may exist instead of one.

(c) The population may not be normal, or (since the data are to a semilog plot in this case) log-normal. There is a great deal written on the question of whether fatigue results are log-normal. A survey seems to suggest that for levels above the

region where the S-N curve flattens out (the endurance limit) the assumption can be permitted. However, Weibull states that when working with practical numbers of test specimens, almost any distribution would do, as it takes 100 tests to determine if it is not log normal, and then to decide which of the remaining three distributions requires "several thousands of tests" (Ref. 35).

During the author's tests, specimen number 67 failed (at level G) at a very low number of cycles. It was decided after due investigation, to consider this a "rare event" (Ref. 34) and to ignore this result.

The Endurance Limit. The statistical difficulties in scatter assessment at or near the endurance limit have often been used as an argument against more specific fatigue requirements by government certifying agencies. Refs. 36, 37 and 38 have proved that the statistical scatter of results stress-wise is not only much more compatible in size, but is also fairly constant over the complete range of cycles. Cycle distribution, on the other hand, presents enormous factors on life and, in the flat region of the S-N curve, sometimes becomes highly skewed and truncated. Factors, even if based on the log of the cycles rather than the cycles alone are unwieldy, and if the greater part of fatigue damage occurs in this region as the linear cumulative damage theory predicts, the shortcomings of a cycles-based factor are obviously intensified.

Static Tests. Most static test results show a normal symmetrical distribution above the specification value, so that in nearly every case (unless an admit-reject system is used, which is not the case in bulk metal processing) there is neither a skew nor a truncated distribution curve for the static strength. Thus, since a normal distribution appears to be the case stress-wise at all cycles, the final ideal fatigue law will probably be amenable to integration with static requirements.

In order to complete the picture of the statistical behaviour of the metal, it was necessary to test as many specimens statically as for any fatigue level. Normal probability when applied to the results gave a population such that there is one chance in a million (with 90% confidence) that a specimen would barely meet the ultimate tensile strength requirement (see Appendix I).

Conclusions

Figs. 13 to 21 show very clearly the reliability of the assumption that a normal distribution is adequate for the distribution of lives at most stress levels. At high levels, however, the results can just be contained in the boundaries of the 90% confidence limit. The results are therefore either no longer normal, or wider confidence limits must be set. The static results shown in Fig. 21 suffer from the difficulty in measuring carefully the ultimate tensile strength with this machine when the results are closely grouped together.

While only nine specimens were inadequate to show the change in the probability curves with stress level, they do serve to show the safety of the confidence method of assessing probability. The 90% confidence values of probability have been calculated for all tests and are used instead of the sample results in this work.

APPENDIX III

Photoelastic Investigation of Three Fillet Shapes

A photoelastic comparison of the radius fillet, the sinusoidal fillet, and the tangent form fillet was undertaken to determine the relative merits of these shapes from the aspects of both efficiency and fatigue. Fatigue crack nucleation seems to be sensitive to stress gradient rather than to stress level. A non-dimensional photoelastic investigation lends itself admirably to such a study.

Test Details

The 0.25 in. thick Araldite models were made from a solution of $9\frac{1}{2}$ to 12 parts hardener, 951 to 100 parts of Araldite 103 by volume, and then filed to shape using metal templates of the fillet shapes. Each model was loaded in tension in a vertical rig, with a load link placed between model and turnbuckle. Sodium light was used as the monochromatic light source. The connections to the model were placed far enough from the fillets to prevent them from causing spurious effects, as can be seen from the photographs.

Each specimen was loaded in stages with a photograph taken at each stage, until the models failed. In this way the maximum number of fringes was obtained whilst avoiding distortion effects prior to failure.

In the analysis the 2.0 in. fillet length is divided into ten stations, each 0.2 in. apart with the station at the beginning of the 1.36 in. diameter section as station 0 and the boundary of the 0.564 in. diameter parallel portion as station 10. Because of the results further stations were taken in the 1.36 diameter section using the same interval and numbered -1, -2, -3, etc. from station 0.

The diameters at each station for each fillet are given in non-dimensional form in Fig. 12. The derivation of the fillet curves is given in Fig. 13.

Results

1. From Figs. 14 and 15 fringe patterns were plotted on graph paper, from which were derived the variations in fringe order along each station. From these, Fig. 19 was obtained, showing the comparative stress-transfer characteristics of the tangent and sinusoidal fillets.

2. It was not possible to obtain more than a single photograph of the radius fillet as the model failed in the connection with the rig (a 0.25 in. diameter pin), at only three fringes. The model was reversed and a photo taken at three fringes (Fig. 16). It then failed again at four fringes. It was not felt advisable to drill a new connection as it would be too close to the fillet.

3. The tangent model exhibited marked edge hardening, which appeared to cause a decrement of one half a fringe. Allowance was made for this in the fringe pattern

plotting.

4. The fringe stress coefficient was 77.5 lb. per inch per order using sodium (5893 Angstrom units). The increment in principal stress was approximately 310 psi per order.

Conclusions

From Fig. 19, the tangent fillet is seen to be quite superior in stress-transfer (following what appears to be the ideal curve for minimizing stress gradient), while the sinusoidal curve possesses a very severe gradient of stress, due to the sharp corner, as the stress falls to zero and then rises again in the wide diameter section.

Moreover, the sinusoidal fillet appears to be a more treacherous configuration as it sets up a disturbed stress pattern past its actual boundary, in the wide diameter region. As it does not begin to act to alter the stress levels until station 7 it cannot but be less efficient in its task if stress gradient rather than stress level is the criterion. While the tangent fillet appears to be heavier than the sinusoidal fillet, the sharp corner of the latter will aggravate the fatigue behaviour of the specimen. In this respect the corner represents a far greater penalty than the added material of the tangent fillet.

The unfortunate failure of the radius fillet prevents a detailed comparison. However, from a study of Figs. 16 to 18, all taken at about the same stage of fringe development, and from other models with radiused fillets, this type usually has low stress corners with a disturbed stress field along the edge in the wide diameter region. However, the radius fillet makes better use of the fillet length, though not as good as with the tangent fillet. In general it appears that the radius fillet falls between the first two. As such it represents an improvement on the sinusoidal form. Becuase of its ease of construction in practical work it is suggested that radius fillets should be used except in fatigue-critical situations where the extra care required in setting up the tangent fillet would be justified.

TABLE 1

BASIC GUST SPECTRUM BY DIFFERENCE

Gust Velocity U fps	Cycles > U	Cycles per U	Gust Velocity U fps	Cycles > U	Cycles per U
0	8,340,000		26		600
.5	7,500,000		26.5	1,600	
1		2,250,000	27		425
1.5	5,250,000		27,5	1,175	
2		1,500,000	28		315
2.5	3,750,000		28.5	860	
3		1,050,000	29		220
3.5	2,700,000		29.5	640	
4		750,000	30		190
4.5	1.950,000		30.5	450	
5		550,000	31		120
5.5	1,400,000		31.5	330	
6		400,000	32		90
6.5	1,000,000		32.5	240	
7		265,000	33		65
7.5	735,000		33.5	175	
8		200,000	34		50
8.5	535,000		34.5	125	
9		145,000	35		34
9.5	390,000		35.5	91	
10		110,000	36		26
10.5	280,000		36.5	65	
11		80,000	37		18
11.5	200,000		37.5	47	
12		55,000	38		13
12.5	145,000		38.5	34	
13		40,000	39		9
13.5	105,000		39.5	25	
14		28,500	40		7
14.5	76,500		40.5	18	
15		18,500	41		5
15.5	58,000		41.5	13	
16		16,000	42		4
16.5	42,000		42.5	9	
17		12,000	43		2.5
17.5	30,000		43.5	6.5	
18		8,000	44		1.75
18.5	22,000		44.5	4.75	
19		6,500	45		1.35
19.5	15,500		45.5	3.4	
20		4,300	46		1
20.5	11,200		46.5	2.4	
21		3,100	47		.6
21.5	8,100		47.5	1.8	
22		2,300	48		.55
22.5	5,800		48.5	1.25	
23		1,600	49		.32
23.5	4,200		49.5	.93	
24		1,200	50		.28
24.5	3,000		50.5	.65	
25		800			
25.5	2,200				

TABLE 2. REDUCTION OF DATA FROM PARTIAL DAMAGE TESTS

(1) Prestress Level Number	(2) Alternating Stress psi	(3) Prestress Cycles n_1	(4) Endurance Linear Extra-polated N_1	(5) Cycle Ratio at Prestress Level n_1/N_1	(6) Mean Endurance at Level E n_2	(7) Cycle Ratio at Level E only n_2/N_E	(8) Total Cycle Ratio $\Sigma \frac{n}{N}$	(9) Damage at Level E 1 - (7)	(10) Exponential in $D = R^x$
1	53,000	.5	1700	.000294	36,250	.616	.616	.384	1/8.5
2	50,000	1	2600	.000385	23,800	.416	.416	.584	1/14.6
3	47,000	2.5	3900	.000640	22,520	.393	.394	.607	1/14.7
4	42,000	10	8000	.001250	57,300	1.000	1.001	0	-
5	37,000	43	10600	.004050	63,760	1.100	1.104	$\doteqdot$ 0	-
6	17,000	15000	270000	.055500	65,780	1.150	1.206	$\doteqdot$ 0	-
7	12,000	72000	520000	.139000	62,000	1.080	1.216	$\doteqdot$ 0	-
8	7,000	370000	1000000	.370000	91,100	1.600	1.970	-.600	-

DAMAGE FOR REGION (1)

(11) Gust Velocity U fps E.A.S.	(12) Cycle Ratio R as (4)	(13) $R^{.10}$ (12)
43	.000660	.480
44	.000550	.472
45	.000450	.463
46	.000385	.458
47	.000335	.450
48	.000307	.445
	Total	2.765

DAMAGE FOR REGION (3)

(14) Gust Velocity U fps E.A.S.	(15) Cycle Ratio R	(16) Exponential $\left(\frac{U}{s} - 1\right)^2$	(17) Healing Cycle Ratio R^y
0	1.000	1	1.000
1	.865	.64	.910
2	.689	.36	.875
3	.552	.16	.942
4	.454	.04	.968
5	.393	0	1.000
6	.333	.04	.957
7	.257	.16	.805
8	.225	.36	.584
9	.191	.64	.345
10	.169	1	.169
		Total	8.555

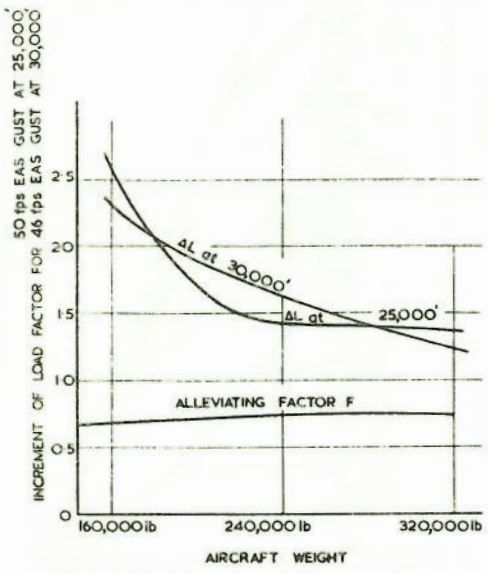

FIG.1. GUST RESPONSE VARIATION PROJECT AIRLINER.

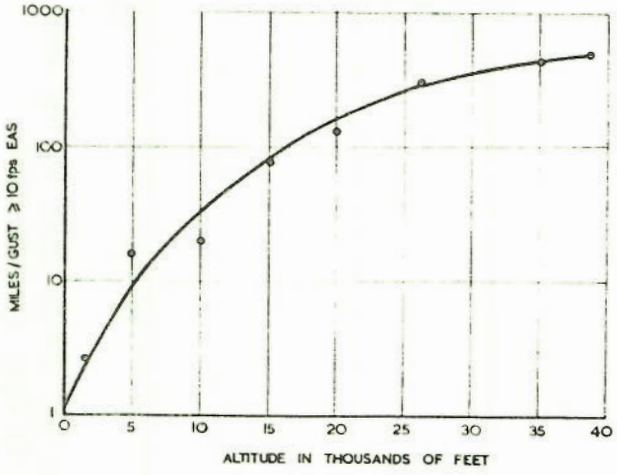

FIG.3. CHANGE IN FREQUENCY OF GUSTS WITH ALTITUDE FOR THE COMET AIRCRAFT.

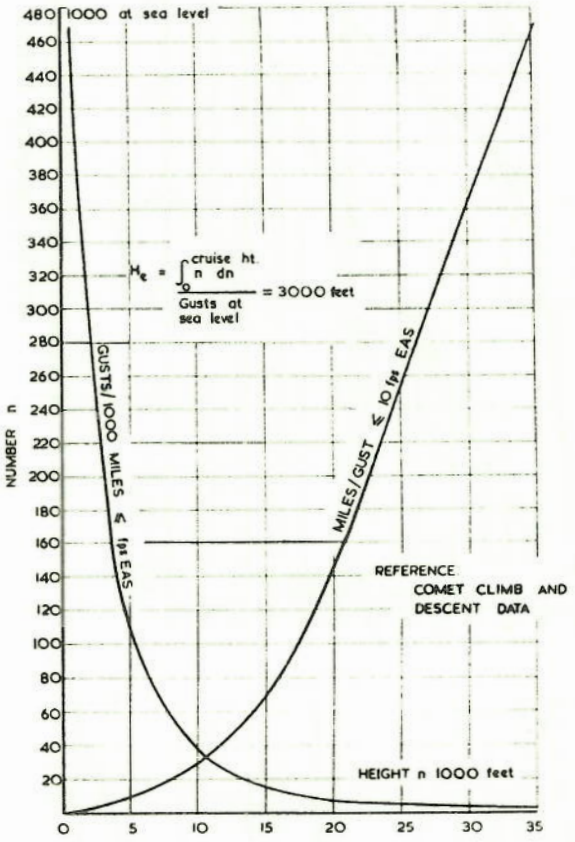

FIG. 2. DERIVATION OF THE EFFECTIVE FATIGUE HEIGHT.

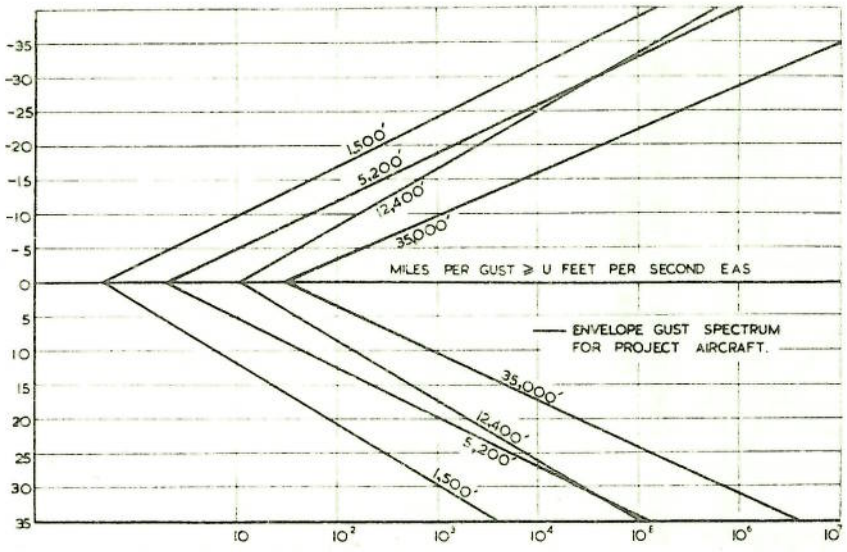

FIG.4. GUST SPECTRA FROM REF 28

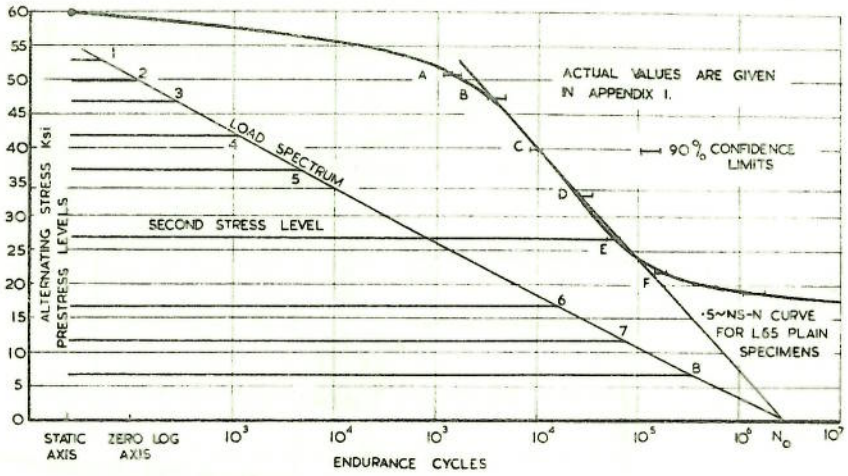

FIG.6. SCHEMATIC LAYOUT OF TWO-LEVEL PARTIAL DAMAGE TESTS.

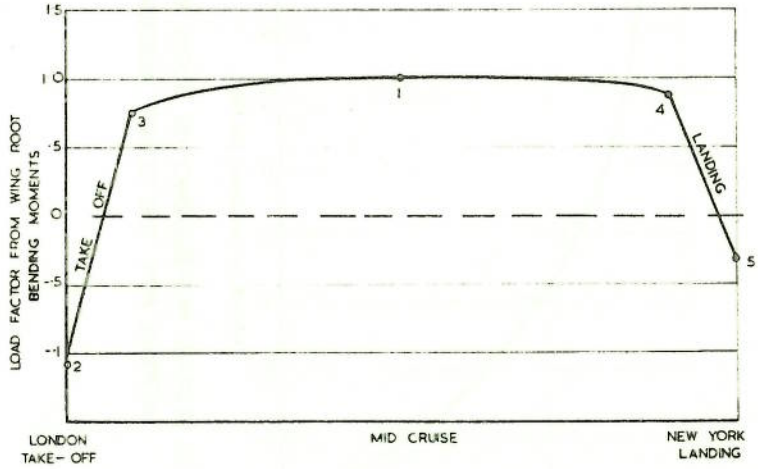

FIG.5. VARIATION IN THE STRESS LEVEL AT THE WING ROOT DUE TO LOAD TRANSFER FROM UNDERCARRIAGE TO WINGS.

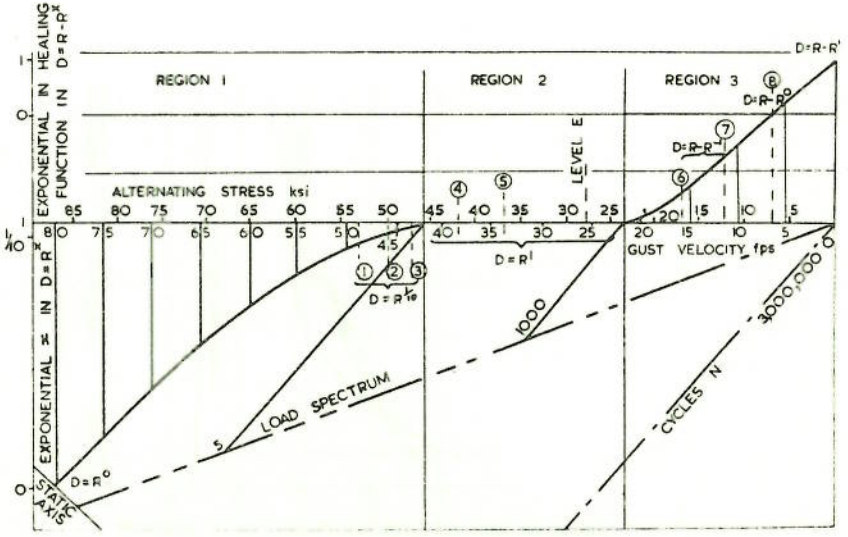

FIG.7. CORRELATION BETWEEN PARTIAL DAMAGE RESULTS AND BEHAVIOR OF THE S-N RELATION.

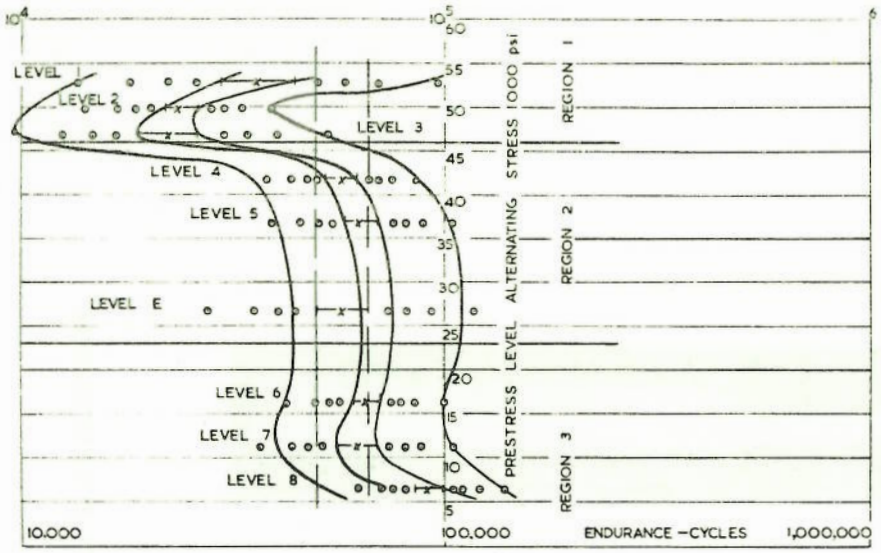

FIG. 8. VARIATION IN ENDURANCE AT LEVEL E FOR PARTIAL DAMAGE TESTS.

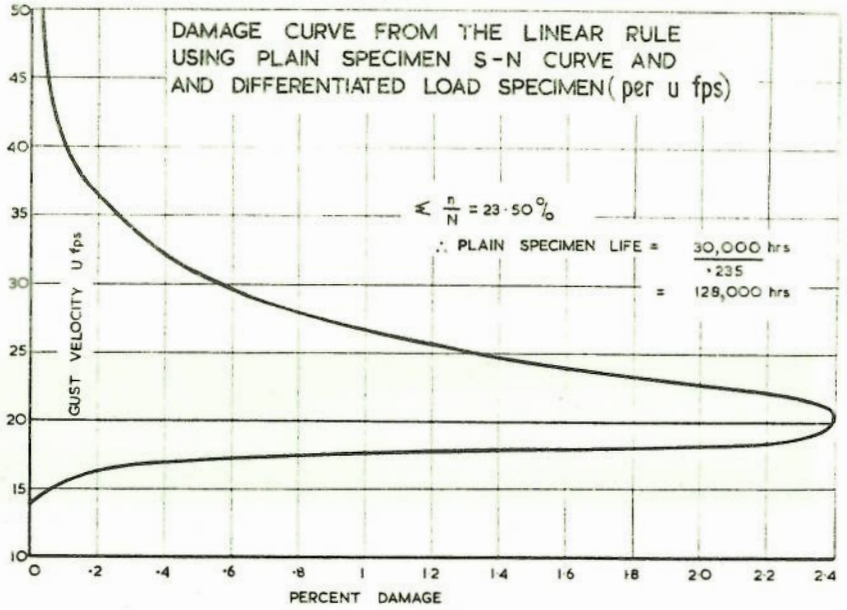

FIG. 9.

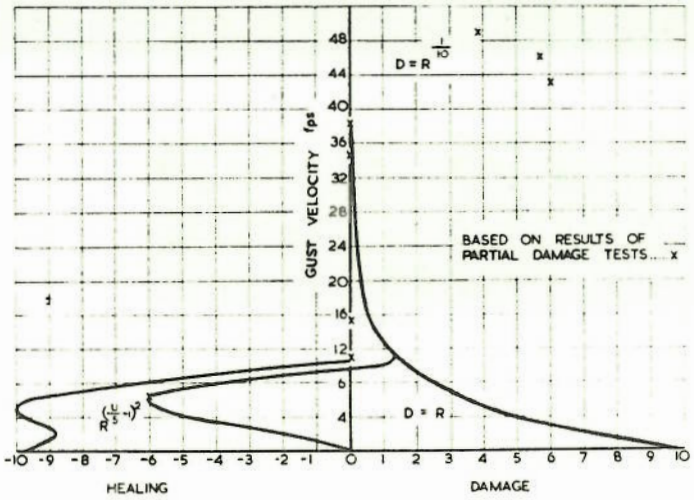

FIG. 10. VARIATION OF DAMAGE ACTIVITY WITH GUST VELOCITY.

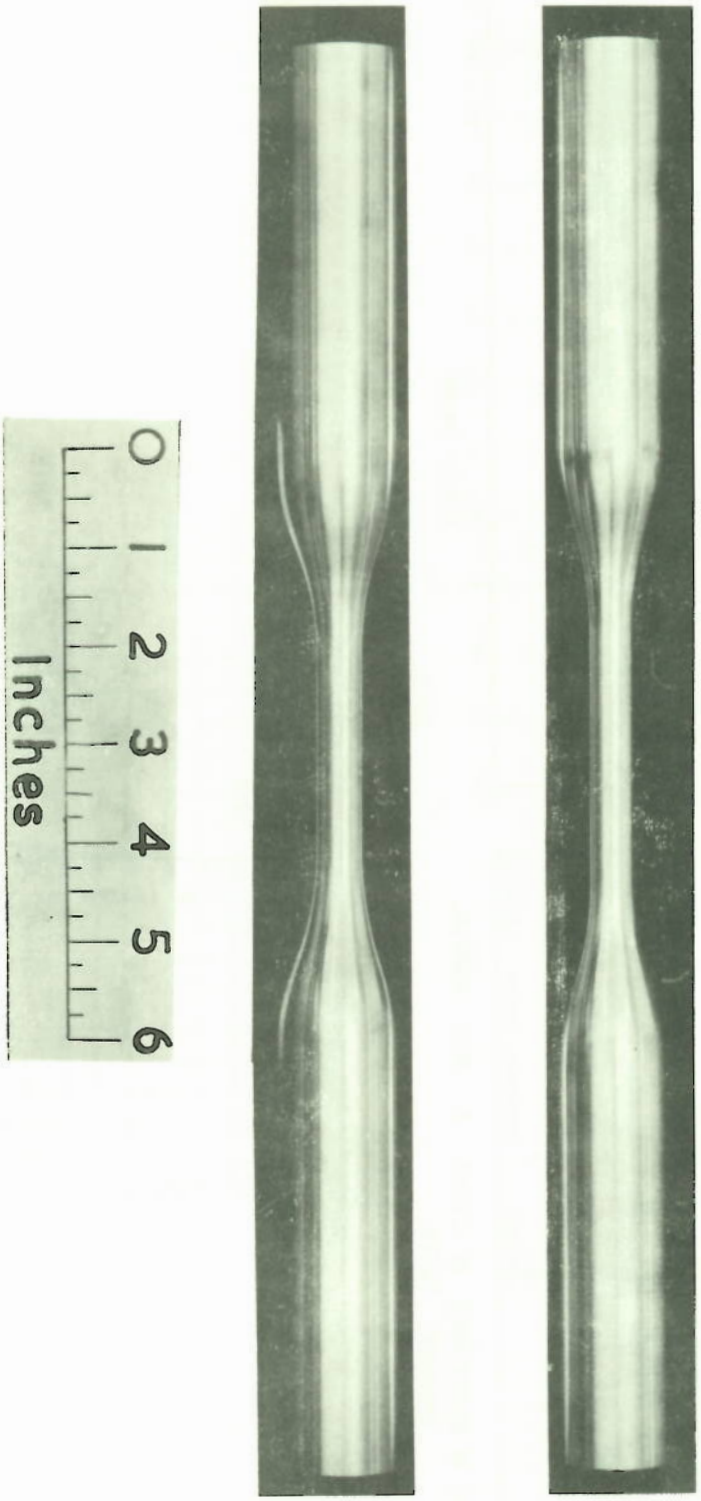

FIG. 11. STATIC AND FATIGUE SPECIMENS

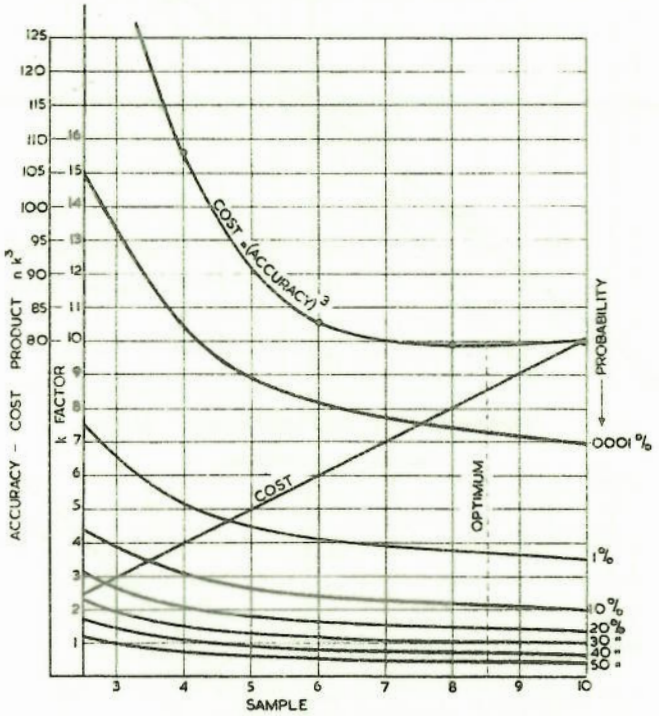

FIG. 12. PLOT OF THE STANDARD DEVIATION FACTOR k FOR A CONFIDENCE OF 90% (REFERENCE FF A REPT 60) WITH 20%, 30% AND 40% P INTERPOLATED (LOGARITHMICALLY)

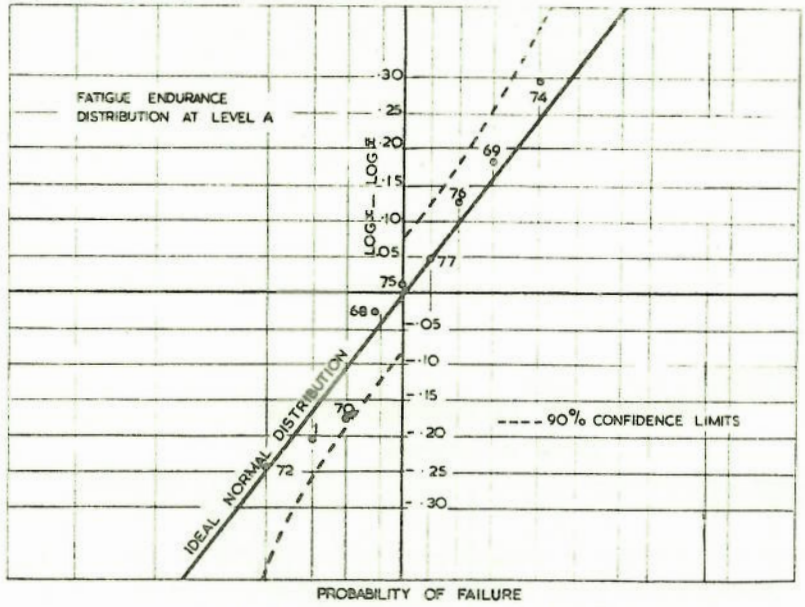

FIG. 13 PROBABILITY OF SURVIVAL

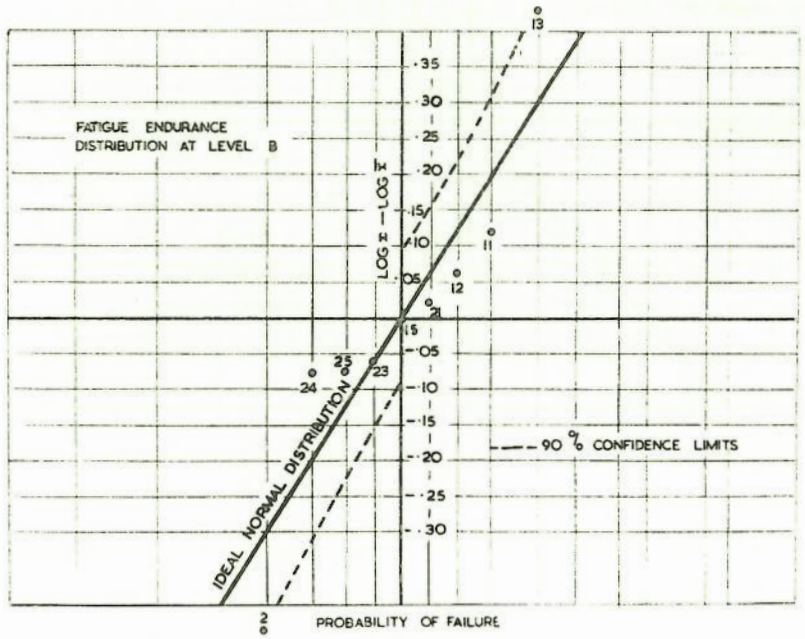

FIG. 14 PROBABILITY OF SURVIVAL.

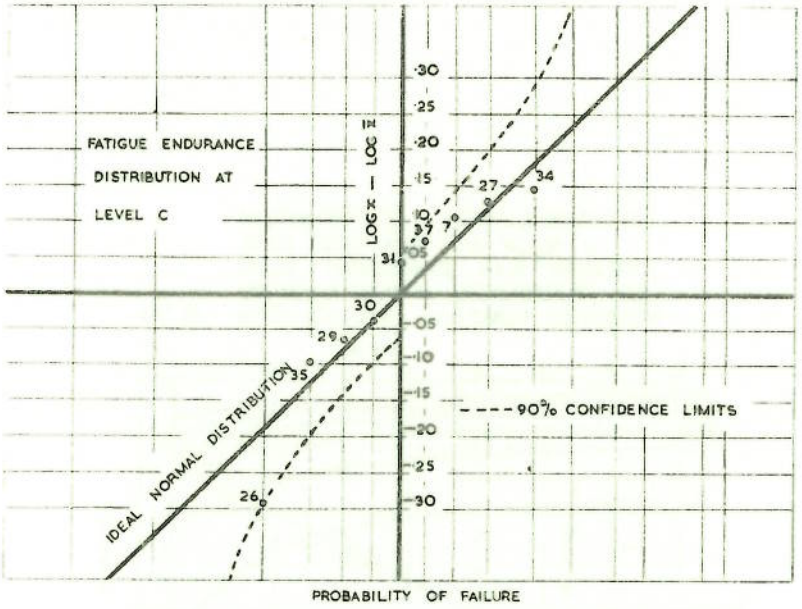

FIG. 15. PROBABILITY OF SURVIVAL

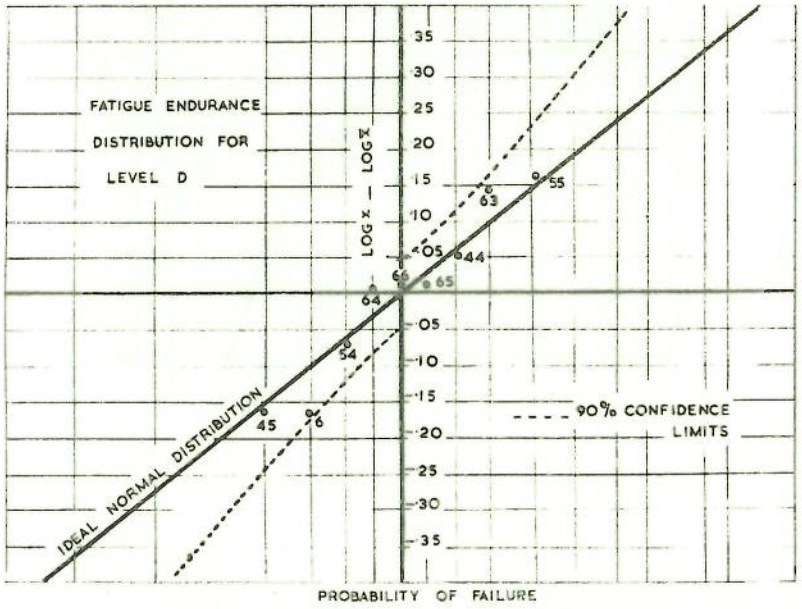

FIG.16 PROBABILITY OF SURVIVAL

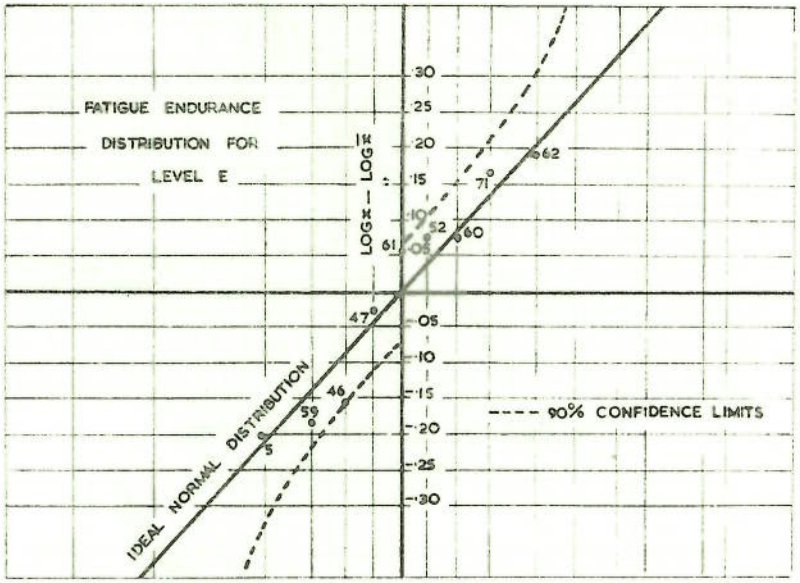

FIG. 17 PROBABILITY OF SURVIVAL

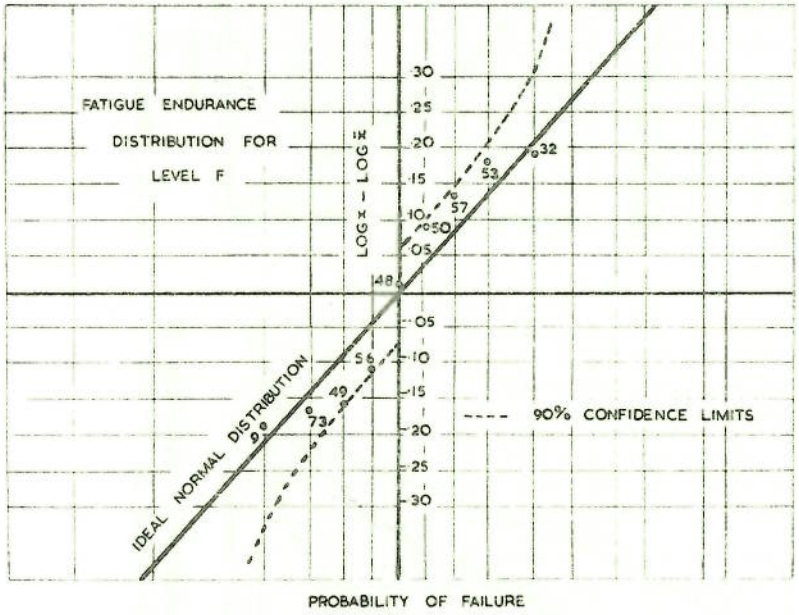

FIG. 18 PROBABILITY OF SURVIVAL

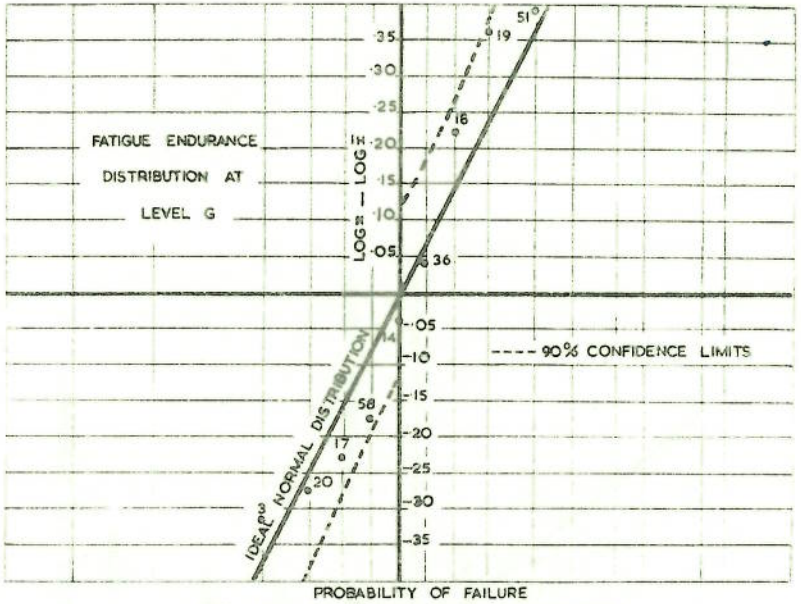

FIG. 19 PROBABILITY OF SURVIVAL

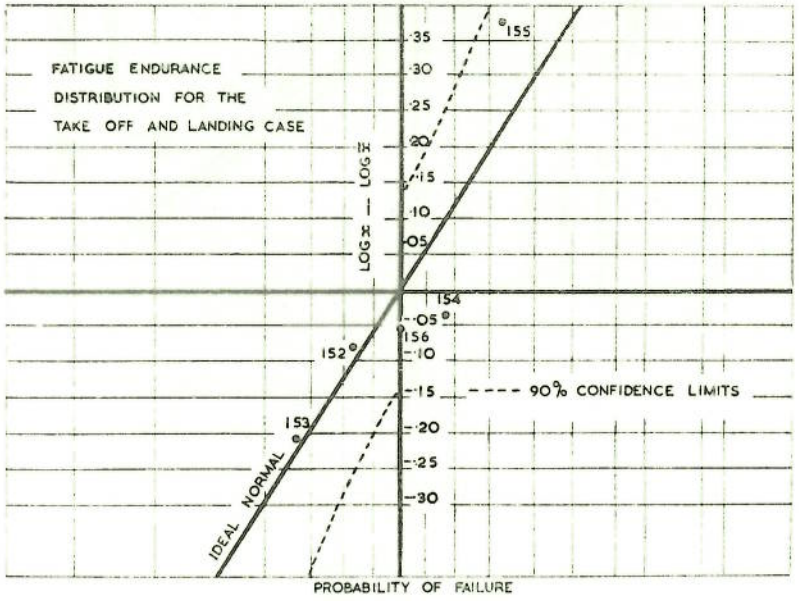

FIG. 20. PROBABILITY OF SURVIVAL

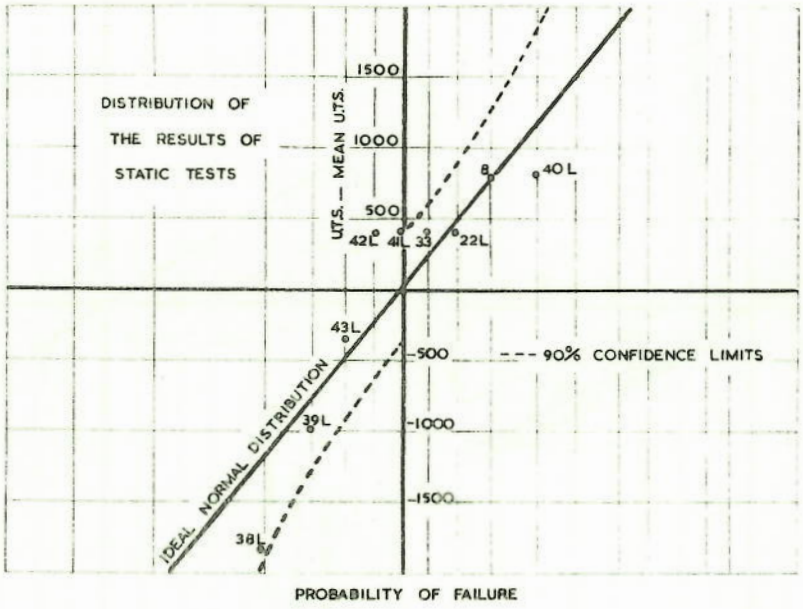

FIG. 21 PROBABILITY OF SURVIVAL

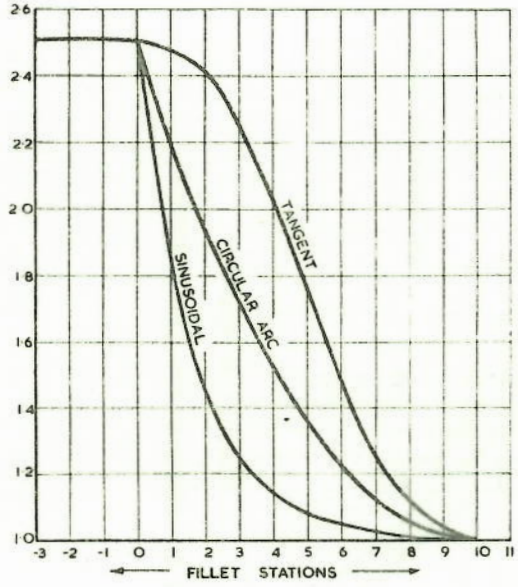

FIG. 22. NON-DIMENSIONAL VARIATION IN DIAMETER BASED ON $l = 564''$.

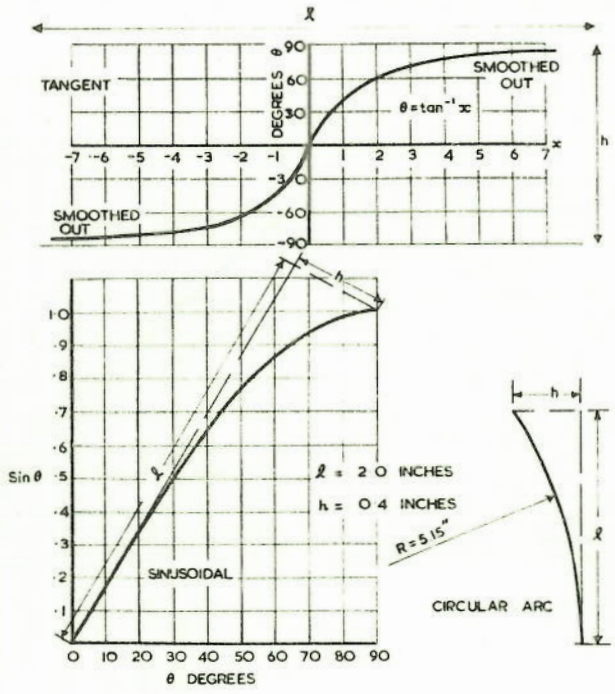

FIG. 23. DERIVATION OF THE FILLET CURVES.

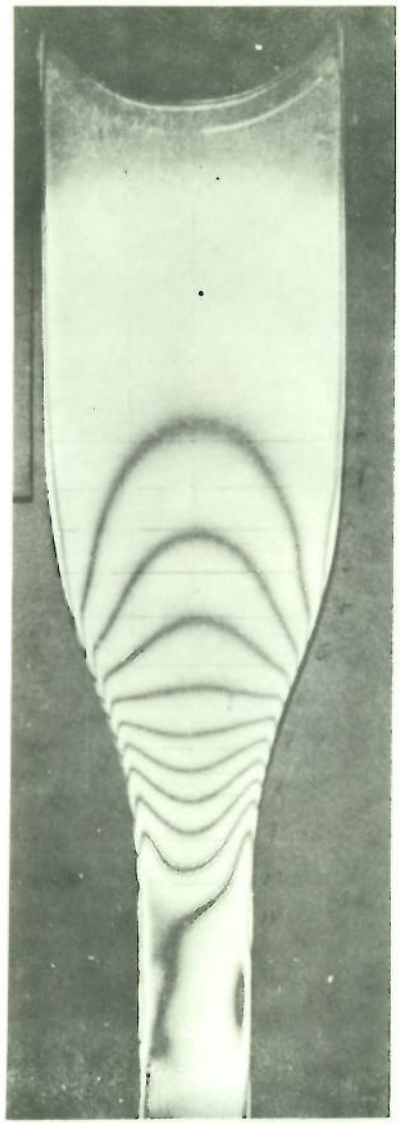

FIG. 24. TANGENT FILLET - n = 15

FIG. 25. SINUSOIDAL FILLET - n = 10

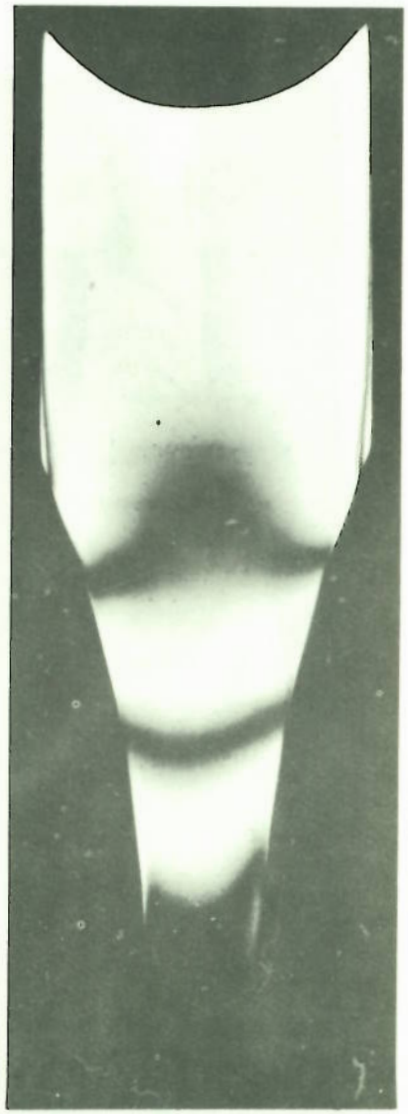

FIG. 26. RADIUS FILLET - n = 3

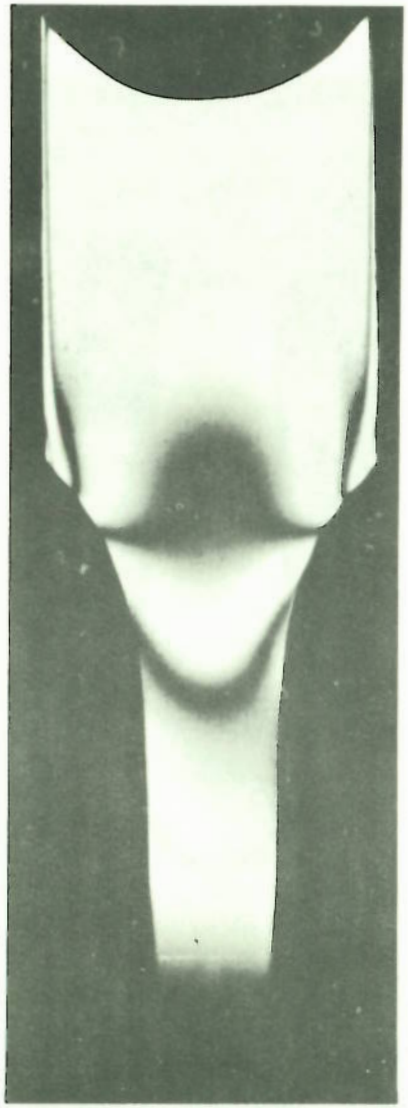

FIG. 27. SINUSOIDAL FILLET - n = 3

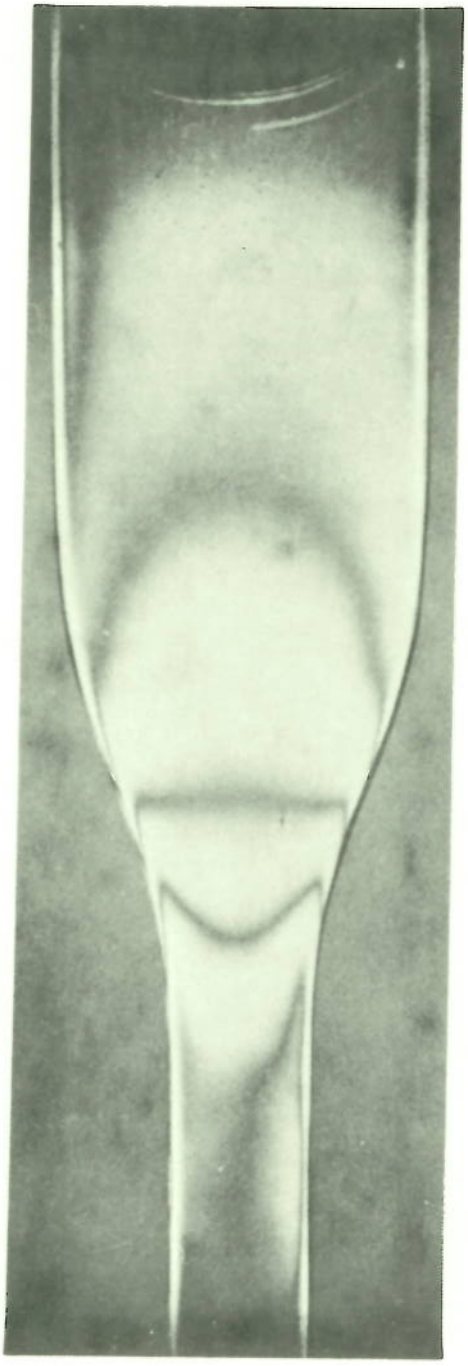

FIG. 28. TANGENT FILLET - n = 5